# Pyroxenites and Megacrysts From Alkaline Melts of the Calatrava Volcanic Field (Central Spain): Inferences From Trace Element Geochemistry and Sr-Nd Isotope Composition

*Carlos Villaseca[1,2]\*, Javier García Serrano[1] and David Orejana[1]*

[1] *Dpt. Mineralogía y Petrología, Facultad CC Geológicas, UCM, Madrid, Spain,* [2] *Instituto de Geociencias IGEO (UCM, CSIC), Madrid, Spain*

Alkaline volcanic rocks from explosive monogenetic centers often carry an unusual cargo of crystals and rock fragments, which may provide valuable constraints on magma source, ascent and eruption. One of such examples is the Cenozoic Calatrava Volcanic Field in central Spain, a still poorly explored area to address these issues. Clinopyroxene, amphibole and phlogopite appear either as megacryst/phenocrysts or forming fine-grained cumulates (pyroxenite enclaves s.l.) in some eruptive centers of this volcanic field. They have previously been interpreted as cogenetic high-P minerals formed within the upper lithospheric mantle. The presence of Fe-Na-rich green and Mg-Cr-rich colorless clinopyroxene types as phenocryst cores or as oscillatory zoned crystals in pyroxenite enclaves points to a complex evolution of mineral fractionates from petrogenetically related magmas. In trace element chemistry all studied clinopyroxene types show parallel rare earth element patterns irrespective of whether they are megacrysts, colorless or green core phenocrysts, or zoned crystals within pyroxenite cumulates. This similarity indicates a genetic relationship between all the fractionated minerals. This is in agreement with the overlapping of initial $^{143}Nd/^{144}Nd$ and $^{87}Sr/^{86}Sr$ ratios of pyroxenite enclaves (0.512793–0.512885 and 0.703268–0.703778) that is within the chemical field of the host magmas and the Calatrava volcanics. The initial $^{143}Nd/^{144}Nd$ and $^{87}Sr/^{86}Sr$ ratios of megacrystic clinopyroxene, amphibole and phlogopite show a more restricted range (0.512832–0.512890 and 0.703217–0.703466), also falling within the isotopic composition of the Calatrava volcanic rocks. Deep magmatic systems beneath monogenetic volcanic fields involve several stages of melt accumulation, fractionation and contamination at variable depths. Trace element and isotope mineral chemistry are powerful tools to understand the history of ascent and stagnation of alkaline basaltic magmas and discriminate between magma mixing, wall-rock contamination and closed magmatic system evolution. In our study, we establish

a cogenetic origin for green and colorless clinopyroxene as high-pressure precipitates from liquids of different fractionation degrees (up to 80%, for the highly evolved melts equilibrated with the green clinopyroxene), originated from a highly solidified front of silica-undersaturated alkaline magmas at mantle reservoirs.

## INTRODUCTION

The study of monogenetic volcanic fields provide important information regarding primary magma genesis, deep-seated differentiation processes and the architecture of the sub-volcanic plumbing systems (e.g. Mattsson et al., 2013; Re et al., 2017). These magmas commonly carry a heterogeneous crystal cargo with complex compositional and textural features, relevant to interpreting the depths and rates of magma storage, transport, fractionation and mixing (e.g. Jankovics et al., 2016). Such data are also useful to understand the mechanisms which trigger volcanic eruption and control its characteristics (Mattsson et al., 2013).

Many monogenetic volcanoes are formed by alkaline rocks which transport mafic megacrysts and ultramafic xenoliths (e.g. Irving and Frey, 1984; Praegel, 1981; Jankovics et al., 2016), whereas pyroxenite enclaves are not so common (Downes, 2007). These enclaves have been interpreted as recycled subducted lithosphere (Allègre and Turcotte, 1986), metasomatic products (Garrido and Bodinier, 1999) or high pressure cumulates (e.g. Bodinier et al., 1987; Wilkinson and Stolz, 1997). When formed by deep-seated fractionation, clinopyroxenite enclaves contain volatile-rich minerals, such as amphibole and phlogopite, and are accompanied by equivalent megacrysts (Orejana et al., 2006 and references therein). Green and colorless anhedral to subhedral phenocryst/megacryst cores can also be found in alkaline volcanic rocks and have been studied in order to unravel their enigmatic origin (e.g. Duda and Schmincke, 1985; Ubide et al., 2014; Jankovics et al., 2016). *In situ* trace element data from such a variety of relic clinopyroxene cores are still sparse and completely lacking in most of the Cenozoic volcanic fields of the Iberian Peninsula, where mafic megacrysts and phenocrysts are common within the pyroclastic deposits of these mafic volcanic centers.

Mafic minerals are important petrogenetic indicators of the evolution of basic-ultrabasic magmas (e.g. Green and Ringwood, 1964; Irving and Frey, 1984; Liotard et al., 1988). Their geochemical composition helps to constrain whether they derive from a common parental melt or from diverse melt batches, and if any genetic affinity is possible between the host volcanic magma and any other melt formed in the context of an active magma plumbing system. A study on the major element geochemistry of mafic megacrysts (clinopyroxene, amphibole and phlogopite) and associated pyroxenite enclaves from two volcanoes of the Calatrava volcanic field was recently published by our research team (Villaseca et al., 2019a). The two host magmas are highly porphyritic, showing a complex crystal population of mafic megacrysts (>5 mm), macrocrysts (5–0.5 mm) and phenocrysts with significant geochemical similarities. Moreover, their major

element composition resembles that of equivalent phases in clinopyroxenite enclaves, suggesting that all of them constitute a cogenetic suite of igneous origin. These fractionates were interpreted as high-P cumulates from mantle magma reservoirs whose rigid chilled margins (solid crusts) were fragmented by subsequent deep $CO_2$ boiling of the fractionated host magmas. The variable crystal cargo dragged by the volcanic magmas (crystals and pyroxenite cumulates) added to variable amounts of peridotite xenoliths entrained from the mantle wall-rocks (Villaseca et al., 2019a).

This work adds new trace element compositional data of minerals (megacrysts, phenocrysts and clinopyroxenite enclaves) within the host alkaline magmas of previously sampled Calatrava volcanoes. We have also determined the whole-rock composition of host rocks and selected clinopyroxenite enclaves along with the Sr-Nd isotope composition of host magmas, pyroxenites and megacrysts. The main objective of this study is to constrain the degree of consanguinity between megacrysts, enclaves and their host magmas and check the previously established cumulate origin. With this objective, our work aims to deepen the understanding of the origin of pyroxenitic and related (mica- and amphibole-rich) cumulates, as well as the generation of diverse types of colored (green to colorless) clinopyroxene pheno-to-megacrysts, in silica-undersaturated alkaline magmas. This work also contributes to a better characterisation of the mantle beneath Central Iberia and to the understanding of differentiation processes operating beneath monogenetic volcanic fields.

## GEOLOGICAL SETTING

The Cenozoic Calatrava Volcanic Field comprises more than 200 monogenetic volcanic centers in an area of around 5500 km$^2$ (Ancochea, 1982). Volcanism in the Calatrava Field took place in two different stages (Ancochea, 1982): (1) a minor ultrapotassic event around 8.7–6.4 Ma and (2) alkaline basalts, basanites and olivine nephelinites and melilitites from 3.7 to 0.7 Ma. The two studied volcanic centers have been recently dated by Ar-Ar on mafic megacrysts yielding ages of 2.2 ± 0.04 Ma (phlogopite from the Cerro Pelado) and 2.8 ± 0.1 Ma (amphibole from the El Aprisco) (Villaseca et al., 2019b). The Pliocene ages of mafic megacrysts from both volcanoes are in agreement with their derivation from the host magmatic systems and represent ages much younger than mantle metasomatic events dated in peridotite xenoliths from the El Aprisco volcano (Villaseca et al., 2019b).

Two volcanoes were sampled due to the common presence of mafic megacrysts and pyroxenite enclaves in their pyroclastic

deposits: the Cerro Pelado scoria cone (olivine nephelinite) and the El Aprisco maar (olivine melilitite) (**Supplementary Figure S1**). The variety and size of these mafic megacrysts are higher in the Cerro Pelado pyroclastic fall deposits than in other Calatrava centers (Villaseca et al., 2019a). Moreover, mantle xenoliths are also present in both volcanoes and they have been described and interpreted as peridotites that have undergone small-to-moderate degrees of partial melting ($\leq 10\%$) (Villaseca et al., 2010). These peridotite xenoliths have been overprinted by different metasomatic agents, mostly alkaline silica-undersaturated melts (Villaseca et al., 2010; Lierenfeld and Mattsson, 2015) but also carbonatite fluids (e.g. González-Jiménez et al., 2014; Villaseca et al., 2019b).

The trace element composition and Sr-Nd isotopic data of primary alkaline magmas suggest that most of the Calatrava volcanics are derived from enriched asthenospheric sources, similar to those defined for the European asthenospheric mantle (Cebriá and López Ruiz, 1995; Granet et al., 1995). Clinopyroxene, amphibole and phlogopite megacrysts are found in different Calatrava volcanoes, but the hydrous mafic megacrysts (amphibole, phlogopite) recorded in the pyroclastic fall deposits of the Cerro Pelado scoria cone outstand by their large size (up to 8.5 cm; Villaseca et al., 2019a). Marginal pyroclastic surge layers of olivine melilitites from the El Aprisco maar also show fragments of clinopyroxene and amphibole megacrysts with a heterogeneous size. Ultramafic clinopyroxene-rich enclaves with variable amounts of hydrous minerals (amphibole and phlogopite), and scarce olivine, can be found associated with these megacrysts in both volcanoes. A rare variety of phlogopite-rich clinopyroxenite (glimmerite, mica > 90 vol%) occurs in the El Aprisco maar (e.g. Villaseca et al., 2019a).

## SAMPLES AND ANALYTICAL METHODS

Four samples were collected from the host mafic rocks. It is important to note that, due to their pyroclastic nature, the bulk of these samples may include contributions from xenoliths (peridotites of mantle derivation and shallow crustal fragments), crystal cargo and hydrothermal alteration. Accordingly, it has been difficult to obtain geochemical data representative of the erupting melts (see also Lierenfeld and Mattsson, 2015). Only one sample from the Cerro Pelado volcanic center (CAL-73) plotted within the main Calatrava volcanic rock data of Cebriá and López Ruiz (1995), whereas the other three (one from El Aprisco and other two from Cerro Pelado) must be considered crystal-contaminated samples. On the other hand, three clinopyroxenite enclaves were also sampled, and there are five additional samples from the Calatrava volcanoes (eruptive centers in **Table 1**).

Whole-rock samples were fused using a lithium metaborate-tetraborate mixture. The melt produced by this process was completely dissolved with 5% $HNO_3$. Major oxide analyses were carried out using a Variant Vista 735 ICP while trace elements were diluted and analyzed by a Perkin Elmer Sciex ELAN 6000 mass spectrometer (ICP-MS) following code 4 Lithoresearch at Activation Laboratories (ACTLABS, Canada).

Relative uncertainties for major elements are bracketed between 1 and 3%, except for MnO (5–10%). The precision for Rb, Sr, Zr, Y, V, Hf and most of the rare earth elements (REE) range from 1 to 5%, and between 5 and 10% for the rest of trace elements. Some samples have concentrations in Pb below detection limits (5 ppm). The precision was evaluated from repeated analyses of the international standards NIST 694, DNC-1, GBW071113, W-2, SY-4, JR-1 and BIR-1a (**Supplementary Table S1**). More information on the procedure, precision and accuracy of ACTLABS ICP-MS analyses can be found at www.actlabs.com. Whole-rock chemical compositions are shown in **Table 1**.

Sr-Nd isotopic ratios were measured on four volcanic rocks (including samples from the Cerro Pelado and El Aprisco host rocks, together with volcanics from other eruptive centers of the Calatrava Volcanic Field), three clinopyroxenites and four mafic megacrysts (**Table 2**) at the Centro de Asistencia a la Investigación (CAI) of Geochronology and Isotope Geochemistry (Complutense University of Madrid, Spain). Whole-rock and megacryst samples were dissolved in ultra-pure reagents and the isotopes were subsequently isolated by exchange chromatography. Isotope analyses were carried out using a Phoenix-IsotopX Multicollector Thermal Ionization Mass Spectrometer with data acquired in multidynamic mode. The analytical procedures used in this laboratory have been described elsewhere (Reyes et al., 1997). Repeated analyses on the NBS-987 standard gave $^{87}Sr/^{86}Sr = 0.710240 \pm 0.00005$ ($2\sigma$, $n = 8$) and for the La Jolla JNdi-1 standard, values of $^{143}Nd/^{144}Nd = 0.512109 \pm 0.000005$ ($2\sigma$, $n = 16$) were obtained (**Supplementary Table S1**). The BHVO-2 standard was also used as internal reference for precision. The $2\sigma$ analytical errors are 0.01% for $^{87}Sr/^{86}Sr$ and 0.006% for $^{143}Nd/^{144}Nd$.

Trace element analysis of mafic minerals (clinopyroxene, amphibole, phlogopite) was performed on the mineral grains previously analyzed by EMP (Villaseca et al., 2019a). Two clinopyroxene and amphibole megacrysts (from each volcanic center) and one phlogopite megacryst (from the Cerro Pelado scoria cone), along with two phenocryst-rich samples (one from each volcano), were selected for trace element analyses (**Supplementary Tables S2, S3**). Two phlogopite-amphibole pyroxenites, one amphibole pyroxenite and a phlogopite-rich (glimmerite) pyroxenite were also used for trace element studies. Trace element mineral compositions were obtained by laser ablation inductively coupled plasma mass spectrometry (LA-ICP-MS) at the Instituto Andaluz de Ciencias de la Tierra (CSIC, UGR, Granada) using a CETAC-Photon Machines 193 nm laser attached to an Agilent 8800 ICP-MS. The diameter of the laser beam was 40 to 60 $\mu$m associated to repetition rates of 10 Hz and laser fluence at the target of ca. 8 J/cm$^2$. A 30 s gas blank was analyzed first to establish the background, followed by 60 s measurements for the remainder of the analysis. Relative element sensitivities were calibrated with a NIST SRM 611 glass standard. Then, each analysis was normalized to Si or Ca using concentrations determined by electron microprobe. Precision and accuracy were assessed from repeated analyses of the USGS-BIR 1G standard and were estimated to be between 2 and 10% for most of the analyzed trace elements.

**TABLE 1 |** Whole-rock major (wt%) and trace element (ppm) composition of the Calatrava Volcanic Field (CVF) rocks.

| Sample | 115605 | 111643 | 111646 | CAL-73 | 114406 | 115271 | 116613 | 117459 | 117460 | 46273* | 115591 | 115601 | 116598 |
|---|---|---|---|---|---|---|---|---|---|---|---|---|---|
| Volcano | Aprisco | C. Pelado | | | Yezosa | C. Gordo | Tormos | Encomienda | | Bienvenida | Aprisco | Aprisco | C. Pelado |
| Rock-type | Melilitite | Nephelinite | | | Nephelinite | Nephelinite | Nephelinite | Melilitite | Melilitite | Melilitite | Clinopiroxenites | | |
| | Crystal-rich | Crystal-rich | Crystal-rich | | | | | | | | | Phl-rich | Phl-rich |
| $SiO_2$ | 42.30 | 39.21 | 46.81 | 41.07 | 40.51 | 41.23 | 39.36 | 34.47 | 35.51 | 37.37 | 38.53 | 40.79 | 42.52 |
| $Al_2O_3$ | 12.31 | 10.33 | 5.73 | 10.61 | 11.22 | 12.82 | 10.60 | 9.15 | 9.90 | 9.31 | 8.84 | 13.05 | 12.40 |
| $Fe_2O_3$ | 11.14 | 12.09 | 8.70 | 12.12 | 12.15 | 13.13 | 12.50 | 11.99 | 13.37 | 12.19 | 18.34 | 11.18 | 9.11 |
| MnO | 0.10 | 0.18 | 0.12 | 0.18 | 0.19 | 0.21 | 0.18 | 0.21 | 0.19 | 0.19 | 0.17 | 0.09 | 0.10 |
| MgO | 14.20 | 13.85 | 20.61 | 11.72 | 10.22 | 8.41 | 12.75 | 10.06 | 11.33 | 13.57 | 9.73 | 12.74 | 13.19 |
| CaO | 10.75 | 11.45 | 15.51 | 13.36 | 15.03 | 12.36 | 13.32 | 17.31 | 16.13 | 15.78 | 13.90 | 11.63 | 13.40 |
| $Na_2O$ | 2.71 | 1.42 | 0.76 | 2.84 | 3.24 | 4.25 | 1.72 | 2.45 | 2.95 | 2.66 | 1.40 | 1.31 | 0.92 |
| $K_2O$ | 1.69 | 1.05 | 0.21 | 0.65 | 1.63 | 2.22 | 0.97 | 1.74 | 2.01 | 1.00 | 0.69 | 2.82 | 2.30 |
| $TiO_2$ | 3.44 | 3.22 | 1.34 | 2.85 | 2.89 | 3.36 | 3.05 | 2.98 | 3.52 | 2.98 | 5.99 | 4.04 | 3.84 |
| $P_2O_5$ | 0.08 | 1.40 | 0.23 | 1.10 | 1.46 | 1.29 | 1.39 | 1.64 | 2.04 | 1.52 | 0.37 | 0.16 | 0.10 |
| LOI | 1.73 | 4.91 | 0.35 | 2.83 | 1.78 | 1.14 | 4.62 | 8.60 | 3.59 | 1.30 | 2.77 | 2.79 | 2.66 |
| Total | 100.40 | 99.12 | 100.40 | 99.32 | 100.30 | 100.40 | 100.50 | 100.60 | 100.60 | 97.87 | 100.70 | 100.60 | 100.60 |
| Sc | 35 | 22 | 44 | 23 | 21 | 21 | 21 | 19 | 20 | 23 | 26 | 33 | 47 |
| V | 302 | 290 | 205 | 250 | 249 | 266 | 269 | 229 | 255 | 266 | 395 | 387 | 314 |
| Cr | 120 | 30 | 1470 | 460 | 360 | 180 | 410 | 470 | 460 | 380 | 30 | 320 | 440 |
| Co | 55 | 56 | 65 | 56 | 50 | 51 | 57 | 45 | 55 | 52 | 52 | 65 | 57 |
| Ni | 160 | 90 | 350 | 250 | 180 | 120 | 290 | 190 | 200 | 250 | 30 | 110 | 180 |
| Ga | 20 | 19 | 9 | 18 | 20 | 21 | 17 | 17 | 20 | 18 | 18 | 21 | 15 |
| Rb | 12 | 6 | 6 | 57 | 38 | 67 | 23 | 33 | 45 | 22 | 5 | 119 | 72 |
| Sr | 388 | 882 | 203 | 2422 | 1383 | 1248 | 1001 | 1082 | 1056 | 1458 | 389 | 348 | 238 |
| Y | 12.1 | 17.7 | 12.1 | 29.5 | 35.8 | 34.5 | 32.9 | 36.7 | 35 | 29.4 | 16.5 | 10.1 | 10.5 |
| Zr | 174 | 240 | 73 | 252 | 345 | 431 | 311 | 328 | 301 | 292 | 244 | 113 | 103 |
| Nb | 24 | 52.5 | 10.9 | 67 | 104 | 118 | 105 | 113 | 98.3 | 96.6 | 44.1 | 18 | 11.1 |

*(Continued)*

**TABLE 1 |** Continued

| Sample | 115605 | 111643 | 111646 | CAL-73 | 114406 | 115271 | 116613 | 117459 | 117460 | 46273* | 115591 | 115601 | 116598 |
|---|---|---|---|---|---|---|---|---|---|---|---|---|---|
| Volcano | Aprisco | C. Pelado | | | Yezosa | C. Gordo | Tormos | Encomienda | | Bienvenida | Aprisco | Aprisco | C. Pelado |
| Rock-type | Melilitite | Nephelinite | | | Nephelinite | Nephelinite | Nephelinite | Melilitite | Melilitite | Melilitite | Clinopiroxenites | | |
| | Crystal-rich | Crystal-rich | Crystal-rich | | | | | | | | | Phl-rich | Phl-rich |
| Ba | 726 | 870 | 152 | 620 | 736 | 954 | 972 | 855 | 534 | 804 | 235 | 915 | 1487 |
| La | 8.45 | 17.2 | 12.2 | 75.3 | 95.7 | 83.6 | 97.6 | 105 | 95.4 | 89.1 | 18 | 12 | 9.22 |
| Ce | 25.1 | 49.2 | 25.8 | 145 | 187 | 165 | 193 | 209 | 200 | 172 | 50.3 | 25.8 | 22.5 |
| Pr | 3.98 | 7.07 | 3.5 | 16.7 | 21.9 | 18.9 | 21.4 | 25.2 | 24.6 | 20.3 | 7.09 | 3.51 | 3.26 |
| Nd | 19.9 | 33.4 | 15.7 | 65.6 | 85.8 | 74.5 | 82 | 92.3 | 93.6 | 76.7 | 31.8 | 16.4 | 15.4 |
| Sm | 5.16 | 7.66 | 3.91 | 12.4 | 15.5 | 13.8 | 14.6 | 16.4 | 17.2 | 13.6 | 7.6 | 4.17 | 4.03 |
| Eu | 1.7 | 2.56 | 1.32 | 3.76 | 4.79 | 4.25 | 4.41 | 5.03 | 5.19 | 4.15 | 2.52 | 1.29 | 1.38 |
| Gd | 4.8 | 6.7 | 3.66 | 9.99 | 12.1 | 11.3 | 11.4 | 13.3 | 13.5 | 10.3 | 6.41 | 3.61 | 3.47 |
| Tb | 0.65 | 0.91 | 0.53 | 1.3 | 1.62 | 1.49 | 1.49 | 1.74 | 1.71 | 1.39 | 0.84 | 0.53 | 0.51 |
| Dy | 3.08 | 4.69 | 2.72 | 6.71 | 7.82 | 7.49 | 7.42 | 8.48 | 8.59 | 6.98 | 4.23 | 2.65 | 2.56 |
| Ho | 0.49 | 0.71 | 0.47 | 1.16 | 1.34 | 1.27 | 1.25 | 1.41 | 1.46 | 1.13 | 0.69 | 0.4 | 0.4 |
| Er | 1.11 | 1.61 | 1.16 | 2.77 | 3.24 | 3.14 | 3.06 | 3.59 | 3.52 | 2.65 | 1.48 | 0.95 | 0.95 |
| Tm | 0.131 | 0.184 | 0.14 | 0.349 | 0.403 | 0.39 | 0.378 | 0.426 | 0.42 | 0.341 | 0.185 | 0.121 | 0.115 |
| Yb | 0.71 | 1 | 0.76 | 2.04 | 2.18 | 2.31 | 2.2 | 2.45 | 2.33 | 1.99 | 1.02 | 0.7 | 0.66 |
| Lu | 0.098 | 0.137 | 0.1 | 0.294 | 0.319 | 0.337 | 0.31 | 0.36 | 0.33 | 0.309 | 0.135 | 0.1 | 0.097 |
| Hf | 5.5 | 6.6 | 2.0 | 5.0 | 5.9 | 7.8 | 5.9 | 5.5 | 5.4 | 5.8 | 6.5 | 2.7 | 3.5 |
| Ta | 2.67 | 4.9 | 0.75 | 5.11 | 6.54 | 7.26 | 6.34 | 7.48 | 7.18 | 6.09 | 4.27 | 1.59 | 0.92 |
| Pb | 24 | <5 | <5 | <5 | <5 | 6 | 7 | <5 | <5 | <5 | 9 | <5 | <5 |
| Th | 0.47 | 1.33 | 1.15 | 9.16 | 9.75 | 9.49 | 13.2 | 9.75 | 8.86 | 9.55 | 1.29 | 0.64 | 0.56 |
| U | 0.15 | 2.66 | 0.36 | 2.08 | 3.04 | 3.03 | 2.35 | 3.57 | 2.76 | 3.4 | 2.46 | 1.9 | 2.38 |
| P (GPa)** | 3.20 | 2.90 | | 2.55 | 2.87 | 2.60 | 2.90 | 4.63 | 5.70 | 4.74 | | | |
| T (°C)** | 1402 | 1305 | | 1309 | 1335 | 1294 | 1328 | 1410 | 1499 | 1460 | | | |

*Analysis from Keenan et al. (2019) **Pressure (P) and temperature (T) estimates of magma segregation from a lherzolitic mantle source (Lee et al., 2009).

**TABLE 2 |** Isotopic (Sr, Nd) composition of the Calatrava Volcanic Field (CVF) rocks and associated megacrysts.

| Sample | Volcano | ($^{87}$Sr/$^{86}$Sr)m | 1 SE | ($^{143}$Nd/$^{144}$Nd)m | 1 SE |
|---|---|---|---|---|---|
| **CVF rocks** | | | | | |
| CAL-73 | C. Pelado | 0.703891 | 0.000003 | 0.512881 | 0.000002 |
| 115271 | C. Gordo | 0.703271 | 0.000002 | 0.512887 | 0.000001 |
| 116613 | Tormos | 0.703477 | 0.000003 | 0.512857 | 0.000001 |
| 117460 | Encomienda | 0.703460 | 0.000002 | 0.512889 | 0.000002 |
| **Clinopyroxenite enclaves** | | | | | |
| 115591 | El Aprisco | 0.703778 | 0.000004 | 0.512793 | 0.000001 |
| 115601 | El Aprisco | 0.703268 | 0.000003 | 0.512883 | 0.000001 |
| 116598 | C. Pelado | 0.703555 | 0.000004 | 0.512885 | 0.000001 |
| **Megacrysts** | | | | | |
| 114403 Phlogopite | C. Pelado | 0.703466 | 0.000003 | 0.512874 | 0.000012 |
| 111653 Amphibole | C. Pelado | 0.703217 | 0.000003 | 0.512855 | 0.000002 |
| 111639 Clinopyroxene | C. Pelado | 0.703243 | 0.000002 | 0.512890 | 0.000002 |
| 114404 Amphibole | El Aprisco | 0.703480 | 0.000002 | 0.512832 | 0.000002 |

# PETROGRAPHY

Below we summarize the textural features of the studied mafic crystals and clinopyroxe-rich enclaves that appear as crystal cargo in alkaline basaltic rocks of the Calatrava Volcanic Field. A detailed petrographic description of the studied samples can be found in Villaseca et al. (2019a).

Clinopyroxene, amphibole and phlogopite megacrysts are single pyroclasts (lapillus) or small fragments in the Cerro Pelado and El Aprisco pyroclastic rocks. Clinopyroxene megacrysts are colorless and mostly unzoned, except for a thin reaction rim with the host magma. In contrast, the Cerro Pelado volcanic rocks show two types of relic clinopyroxene phenocryst cores: (1) anhedral green and (2) anhedral to euhedral colorless. In the El Aprisco maar only the second type of relic clinopyroxene core (colorless) was observed. Both phenocryst cores develop pale purple rims petrographically similar to melilitite/nephelinite groundmass clinopyroxene (**Figures 1A,C**). Amphibole makes up the largest megacrysts (up to 8.5 cm in the Cerro Pelado volcano), and phlogopite is usually unzoned and no larger than 4.5 cm. Most megacrysts display reaction rims or corrosion gulfs.

The studied pyroclastic rocks also include small black and elongated enclaves that can be classified as amphibole clinopyroxenite, amphibole-phlogopite clinopyroxenite, phlogopite clinopyroxenite and glimmerite (>90% phlogopite) (Villaseca et al., 2019a). Their size ranges from 1 to 7 cm. They show mostly medium- to fined-grained equigranular texture (**Figure 1B**). Pyroxenites lack typical metamorphic textures, which is indicative of a recent magmatic origin before volcanic entrainment. Clinopyroxene can be colorless or pale green and appear mutually intergrowing as complex oscillatory zoned crystals (**Figure 1D**), mantled by an external discordant thin purple rim, suggesting a genetic link with the two types of phenocryst cores described in the nephelinite from the Cerro Pelado cone. Amphibole shows slight zoning in the form of irregular patches. Occasionally, phlogopite may show kinked textures in the glimmeritic enclaves, likely associated to flowage and collisions with the conduit walls during ascent (Peterson

and LeCheminant, 1993). The studied volcanic rocks also include a varied xenocryst population from the fragmentation of mantle xenoliths (e.g. Fo-rich olivine, orthopyroxene and Al-Mg-rich spinel).

# WHOLE-ROCK GEOCHEMISTRY OF VOLCANIC HOST ROCKS AND PYROXENITE ENCLAVES

Although studied volcanic rocks have been classified as melilitites (El Aprisco) or nephelinites (Cerro Pelado) by petrographic means (Ancochea, 1982), their variable silica and alkali contents causes them to plot in the foidite, basanite and basalt fields when using the TAS diagram (**Figure 2A**). The complexity of sampling pyroclastic rocks representative of the transporting melt is evident, as they appear as mingled rocks comprising a mixture of crystal cargo (phenocrysts, fragmented antecrysts, xenoliths), juvenile material and accidental crustal lithics (see also Lierenfeld and Mattsson, 2015). Previous attempts to record the original composition of host magma that transported such a great quantity of solid cargo failed to reproduce the melilitic or nephelinitic original character of the volcanic host (Lierenfeld and Mattsson, 2015). In this work, only sample CAL-73 from the Cerro Pelado nephelinite volcano (sample provided by J.M. Cebriá) yields a consistent composition when compared to other nephelinites from the Calatrava Field (**Figure 2**; **Table 1**). Most crystal-rich samples from these volcanoes have low alkali contents and plot outside the typical compositional field of Calatrava volcanic rocks (**Figure 2A**). On the basis of the silica-undersaturated diagram of Le Bas (1989), studied rocks of the two volcanoes (including pyroxenites) plot in the nephelinite field (**Figure 2B**). The higher MgO contents (>13.8 wt%, **Table 1**) of phenocryst-rich rocks of these two volcanic centers, with respect to other Calatrava volcanic rocks (mostly in the range of 8.4 to 12.8 wt%) are likely related to the relative abundance of mafic crystal cargo (clinopyroxene, olivine, amphibole and phlogopite). When using binary major
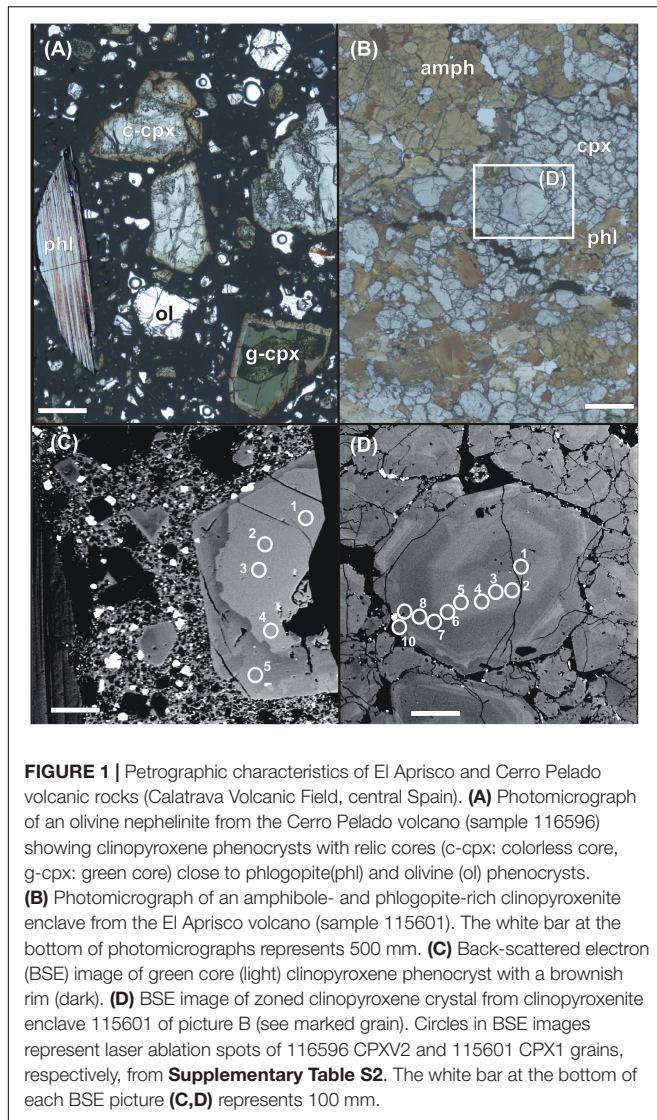
FIGURE 1 | Petrographic characteristics of El Aprisco and Cerro Pelado volcanic rocks (Calatrava Volcanic Field, central Spain). **(A)** Photomicrograph of an olivine nephelinite from the Cerro Pelado volcano (sample 116596) showing clinopyroxene phenocrysts with relic cores (c-cpx: colorless core, g-cpx: green core) close to phlogopite(phl) and olivine (ol) phenocrysts. **(B)** Photomicrograph of an amphibole- and phlogopite-rich clinopyroxenite enclave from the El Aprisco volcano (sample 115601). The white bar at the bottom of photomicrographs represents 500 mm. **(C)** Back-scattered electron (BSE) image of green core (light) clinopyroxene phenocryst with a brownish rim (dark). **(D)** BSE image of zoned clinopyroxene crystal from clinopyroxenite enclave 115601 of picture B (see marked grain). Circles in BSE images represent laser ablation spots of 116596 CPXV2 and 115601 CPX1 grains, respectively, from **Supplementary Table S2**. The white bar at the bottom of each BSE picture **(C,D)** represents 100 mm.

element diagrams, most of the Calatrava volcanic rocks define a broad trend that might be induced by operation of minor fractional crystallization processes (Cebriá, 1992; **Figure 2**). In these diagrams, pyroxenites usually plot defining contrasted evolution lines or they are clearly outside of the main Calatrava compositional field (**Figures 2C,D**, respectively). Pyroxenite composition seems to be mainly controlled by mafic phases, especially by clinopyroxene or amphibole chemistry.

Major and trace element variation diagrams for pyroxenites and host-rocks display a marked data scatter, but in some diagrams, a clear distinction is drawn between pyroxenites and host magma compositional fields (**Figures 2, 3**). Pyroxenites have markedly low contents of Na, P, Nb, Ta, Th, U, Zr, Hf, LILE (except for K, Rb and Ba in phogopite-bearing types: 115601, 116598), Cr, Ni, and REE-Y (**Figure 3**). On the contrary, phlogopite-bearing pyroxenites are markedly rich in Al, K, Ti, Rb, Ba and Sc-V. Phlogopite-rich pyroxenites also display higher $SiO_2$, $Al_2O_3$ contents than the variety without mica (**Table 1** and

**Figure 2C**). Most of the chemical features of pyroxenites seem to be controlled by the combination of their mafic phases and Fe-Ti-rich minerals (Ti-magnetite, ilmenite, titanite). Pyroxenites in most trace element diagrams plot outside the compositional field of Calatrava volcanic rocks (**Figure 3**).

In chondrite normalized REE patterns all the pyroxenites show a similar pattern, with a mostly flat LREE pattern and a steeper shape from Eu to Lu (**Figure 4**). On the contrary, melilitites/nephelinites of the Calatrava Field (including sample CAL-73 from El Aprisco) exhibit a significant homogeneity in composition, displaying a strongly fractionated REE pattern (**Figure 4**). The analyzed pyroxenites show marked negative anomalies in Th, Nb (Ta) and P (and positive in Ti), contrasting with the patterns of the Calatrava volcanic rocks. Phlogopite-bearing pyroxenites show slightly positive Rb, Ba and K anomalies (**Figure 4**). The CAL-73 sample and other Calatrava rocks show a similar pattern when compared to the Late-rift volcanic rocks of the Neogene Bohemian Massif, with characteristic negative anomalies in K and Zr and positive anomalies in P (Ulrych et al., 2011).
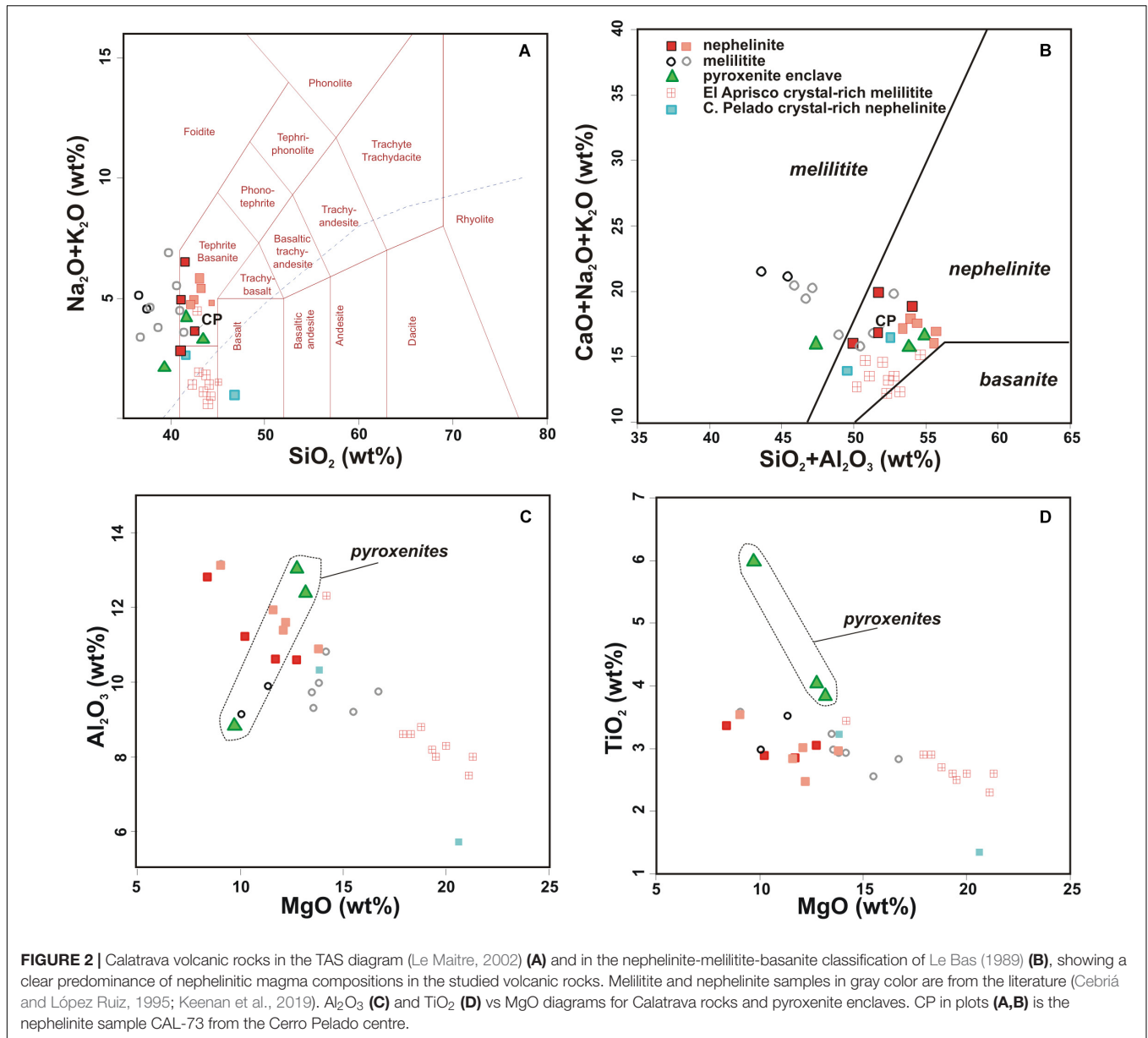
The Sr and Nd isotopic composition of pyroxenites and the Calatrava volcanic rocks fall in the same range of 0.703270–0.703890 and 0.512790–0.512890, plotting close to the HIMU and FOZO components, and overlapping the EAR, common asthenospheric mantle reservoir of the circum-Mediterranean area (**Figure 5** and **Table 2**). This good fitting in isotopic composition suggests that the pyroxenite cumulates likely crystallized directly from magmas cogenetic with the host volcanic melts.

## TRACE ELEMENT AND Sr-Nd ISOTOPE GEOCHEMISTRY OF MEGACRYSTS-PHENOCRYSTS

### Clinopyroxene

Clinopyroxene megacrysts show Mg# values [(MgO/(MgO+FeOt) on a molecular basis] that are indicative of a primitive composition, with only a minor variation between volcanoes (0.81–0.83 in El Aprisco and 0.83–0.84 in Cerro Pelado) (Villaseca et al., 2019a). Two types of phenocryst cores appear in the Cerro Pelado volcanics: colorless and green clinopyroxenes. They show a contrasted composition, with the green cores exhibiting lower Mg#, $TiO_2$ and $Al_2O_3$, and higher FeO and $Na_2O$ contents than the colorless clinopyroxene (Villaseca et al., 2019a).

The trace element composition of clinopyroxene megacrysts, plotted on chondrite- and primitive mantle-normalized diagrams, displays a relatively uniform pattern in both volcanic centers, although slightly higher contents can be found in megacrysts from the El Aprisco melilitite (**Figure 6**). They all present characteristic convex-upward LREE patterns, with strong depletion in the HREEs and negative anomalies in Rb-Ba, K, Pb and P (**Figures 6A,B**). The colorless cores of clinopyroxene phenocrysts exhibit an overlapping composition with respect to megacrysts (**Supplementary Table S2** and **Figure 6C**). This feature suggests a genetic connection between

**FIGURE 2 |** Calatrava volcanic rocks in the TAS diagram (Le Maitre, 2002) **(A)** and in the nephelinite-melilitite-basanite classification of Le Bas (1989) **(B)**, showing a clear predominance of nephelinitic magma compositions in the studied volcanic rocks. Melilitite and nephelinite samples in gray color are from the literature (Cebriá and López Ruiz, 1995; Keenan et al., 2019). Al₂O₃ **(C)** and TiO₂ **(D)** vs MgO diagrams for Calatrava rocks and pyroxenite enclaves. CP in plots **(A,B)** is the nephelinite sample CAL-73 from the Cerro Pelado centre.
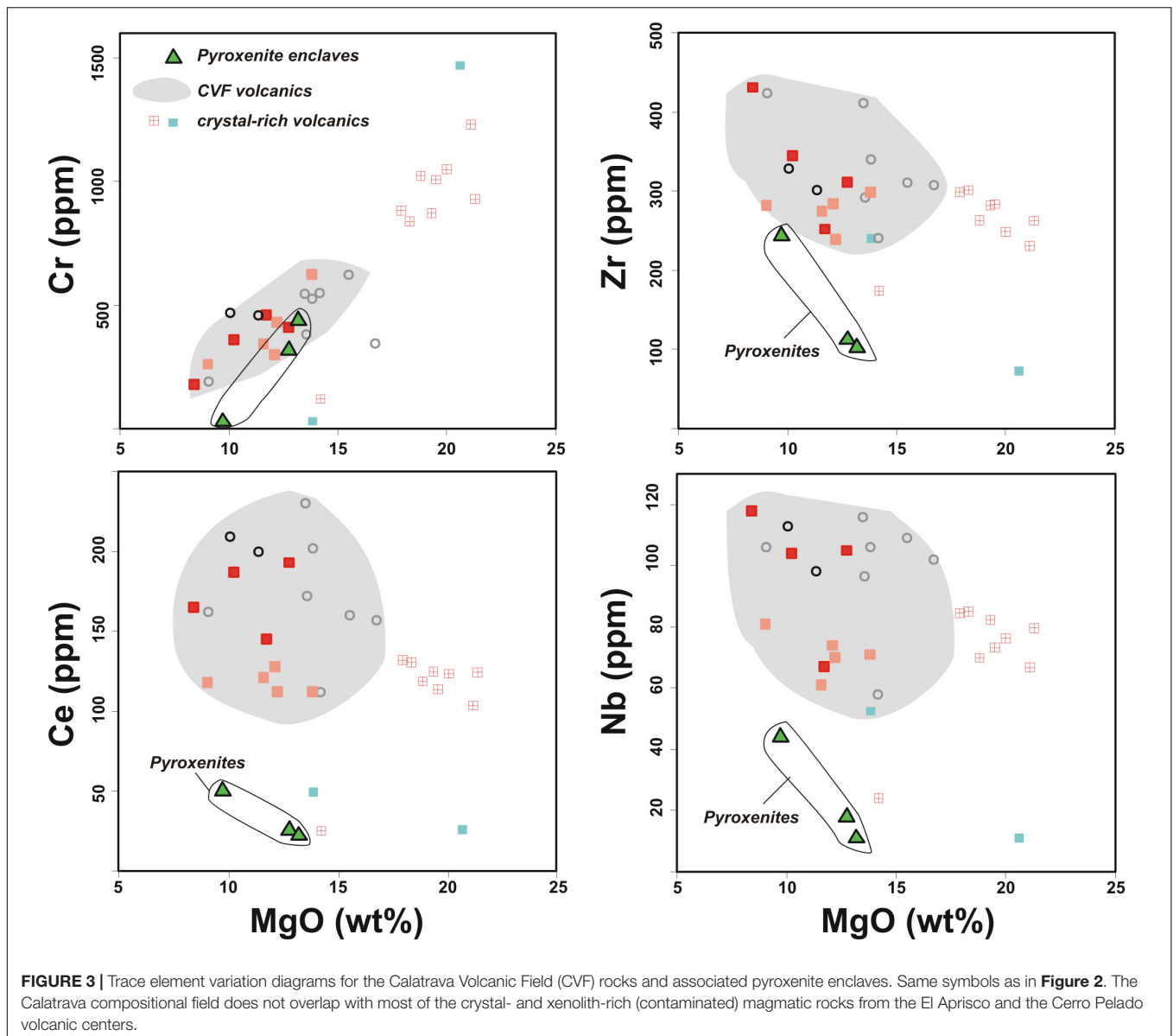
both types of crystals. The trace element chemistry of these Calatrava clinopyroxene megacrysts-phenocrysts is very similar to that described in types II and III of megacrysts from the Eifel (Shaw and Eyzaguirre, 2000) but is clearly different to the xenocrystic cores of phenocrysts in alkaline basalts from the Carpathian-Pannonian region (Jankovics et al., 2016).

The green core phenocrysts show REE patterns parallel to those from colorless megacrysts and phenocrysts (**Figure 6**C), reinforcing the cogenetic character of all studied clinopyroxene types. Nevertheless, the green cores have higher REE, Zr-Hf and Nb-Ta and lower Ti-Cr-Ni contents than colorless clinopyroxenes (**Figures 6C,D**, **7**). The chemistry of purple rims around green and colorless phenocryst cores, showing intermediate values in Mg# and Ni (Cr) (**Figure 7**), suggests that the host magma that transported the crystal cargo might have an

intermediate chemical composition between those deep magmas that originated both phenocryst core types. Nevertheless, the wide REE and other incompatible trace element contents shown by purple clinopyroxene rims (**Figures 6G,H**) suggests a complex melt evolution of the host magma during volcanic emplacement.

## Amphibole

The amphibole megacrysts found in the Cerro Pelado and El Aprisco volcanoes constitute a homogeneous group displaying a moderate chemical variation (Villaseca et al., 2019a). Amphibole Mg# may reach high values (up to 0.83), which is indicative of a fairly primitive composition and is positively correlated with Al₂O₃ and K₂O (Villaseca et al., 2019a). Patchy zoning and smaller amphibole crystals can be observed occasionally within

**FIGURE 3 |** Trace element variation diagrams for the Calatrava Volcanic Field (CVF) rocks and associated pyroxenite enclaves. Same symbols as in **Figure 2**. The Calatrava compositional field does not overlap with most of the crystal- and xenolith-rich (contaminated) magmatic rocks from the El Aprisco and the Cerro Pelado volcanic centers.
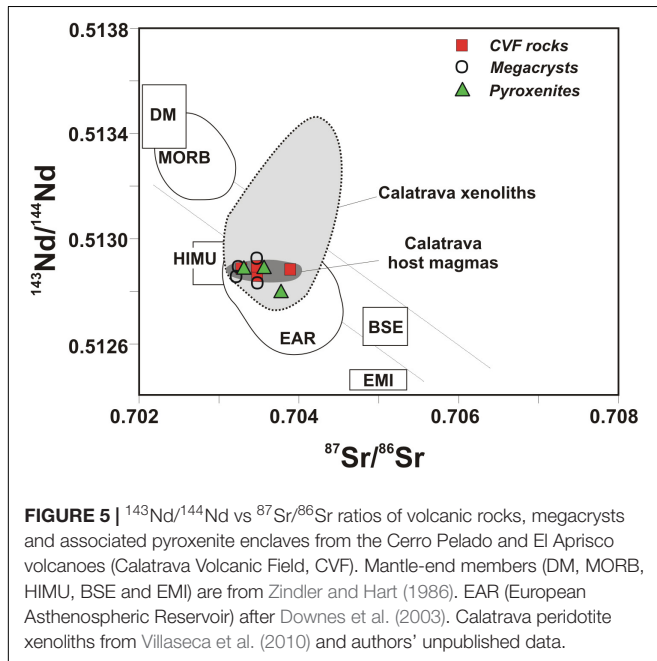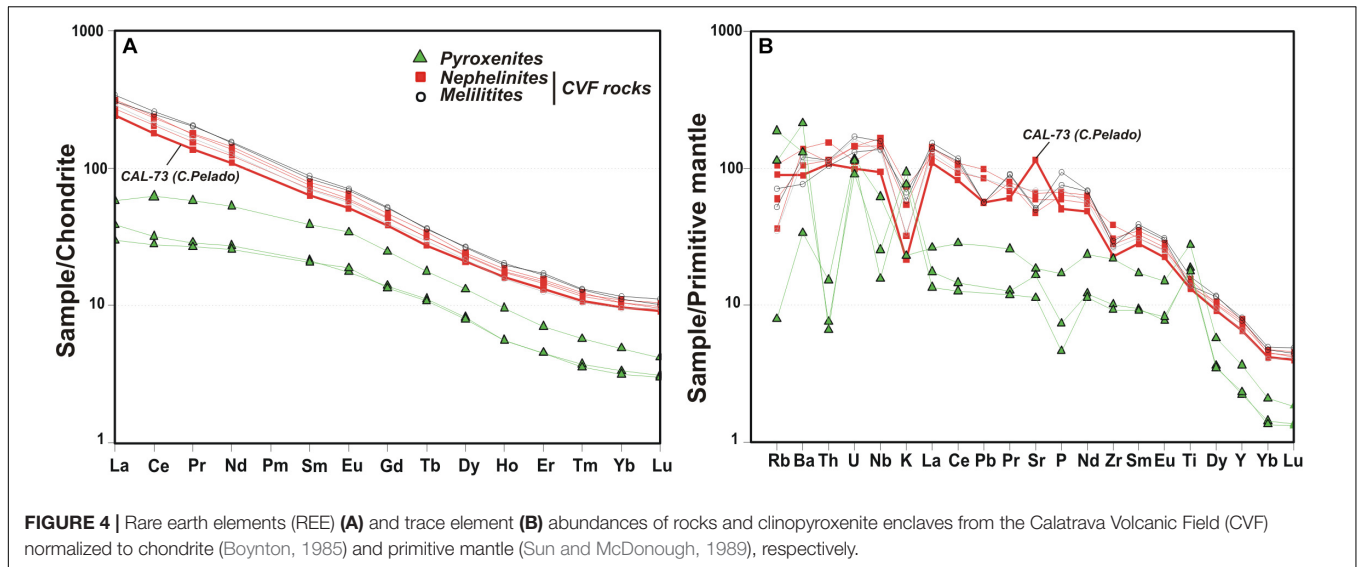
megacrysts. Amphibole phenocrysts have never been found in the studied pyroclastic rocks of these two volcanoes.

The amphibole megacrysts exhibit a REE pattern similar to that of clinopyroxene megacrysts, characterized by a convex-upward shape for the LREE and depleted HREE (**Figure 8A**). Nevertheless, amphibole primitive mantle-normalized patterns are very different to those of clinopyroxene due to its higher LILE (K, Rb, Ba > Sr), Nb-Ta and Pb contents (**Figure 8B**). The trace element chemistry of the Calatrava amphibole megacrysts (**Supplementary Table S3**) is very similar to that described in megacrysts from the Eifel (Shaw and Eyzaguirre, 2000) or from the Bohemian Massif (Mayer et al., 2014; Ulrych et al., 2018), as was the case of clinopyroxenes. Moreover, the $D^{amp/cpx}$ (REE,Th,U, Zr and Hf) estimated for both mineral megacrysts are in the range of 0.6–2, which is very similar to the values obtained from natural rocks and experimental data (Chazot et al., 1996;

Grégoire et al., 2000; Raffone et al., 2009; Ubide et al., 2014), indicating the approach of chemical equilibrium between them.

## Phlogopite

The major element composition of phlogopite megacrysts, phenocrysts and microinclusions in other mafic megacrysts of the Cerro Pelado volcano defines a narrow chemical variation (Figure 9 of Villaseca et al., 2019a). These phlogopites exhibit a fairly primitive composition, with Mg# ranging mostly from 0.85 to 0.78 and high $Al_2O_3$ (15.6–17.4 wt%), $TiO_2$ (4.4–6.5 wt%) and $K_2O$ (7.5–10 wt%) concentrations. $Cr_2O_3$ contents are lower than 0.2 wt% in all cases. The close resemblance in major element composition between microinclusions and larger crystals (megacrysts and macrocrysts) was interpreted as their derivation from a common magma batch (Villaseca et al., 2019a).

**FIGURE 4 |** Rare earth elements (REE) **(A)** and trace element **(B)** abundances of rocks and clinopyroxenite enclaves from the Calatrava Volcanic Field (CVF) normalized to chondrite (Boynton, 1985) and primitive mantle (Sun and McDonough, 1989), respectively.



**FIGURE 5 |** $^{143}Nd/^{144}Nd$ vs $^{87}Sr/^{86}Sr$ ratios of volcanic rocks, megacrysts and associated pyroxenite enclaves from the Cerro Pelado and El Aprisco volcanoes (Calatrava Volcanic Field, CVF). Mantle-end members (DM, MORB, HIMU, BSE and EMI) are from Zindler and Hart (1986). EAR (European Asthenospheric Reservoir) after Downes et al. (2003). Calatrava peridotite xenoliths from Villaseca et al. (2010) and authors' unpublished data.

$D^{Phl/Amp}$ for Nb-Ta (0.5–0.6), Zr-Hf (0.06–0.12), Rb (16–20), Ba (8–9) and Sr (0.3–0.4) are broadly similar to those reported in other studies (Grégoire et al., 2000; Kaczmarek et al., 2016).

Regarding the isotopic composition, the four analyzed megacrysts (two amphiboles from both volcanic centers and the phlogopite and clinopyroxene from the Cerro Pelado volcano) (**Table 2**) yield similar $^{87}Sr/^{86}Sr$ (0.703217–0.703480) and $^{143}Nd/^{144}Nd$ ratios (0.512832–0.512890) and plot within the wider isotopic field of the Calatrava volcanic rocks (**Figure 5**). These isotopic signatures suggest that the studied mafic megacrysts crystallized from melilititic-nephelinitic melts are similar in composition to their host magmas.

## TRACE ELEMENT GEOCHEMISTRY OF PYROXENITE MINERALS

The composition of clinopyroxene from the pyroxenite enclaves overlaps the field of megacrysts, although defining a wider range for the REE contents, plotting toward either more enriched but also less differentiated compositions (**Figures 6E–F**). The two clinopyroxenites included in pyroclasts from the El Aprisco maar, which show colorless-greenish zoned crystals, have the lowest (sample 115591) and highest (sample 115601) REE contents of all the studied high-P clinopyroxenes (**Figure 6E**).

Zoning profiles in these clinopyroxenes were previously characterized by the alternation of Si–Mg- and Fe–Al–Ti–Na-rich bands (Villaseca et al., 2019a). With respect to trace element contents, the green bands (**Figure 1D**) have slightly higher P, REE, Y, Th, U, Nb and Ta contents than the colorless ones (**Figure 9**). This chemical contrast is smaller than that shown by green and colorless phenocryst cores, at least for some elements (e.g. Zr, Sc, Cr and Ni) (**Figures 6**, **7**). In any case, the similarity in composition of the colorless phenocryst cores, megacrysts and most clinopyroxenes from the pyroxenite enclaves is remarkable. Similarly, some greenish clinopyroxene
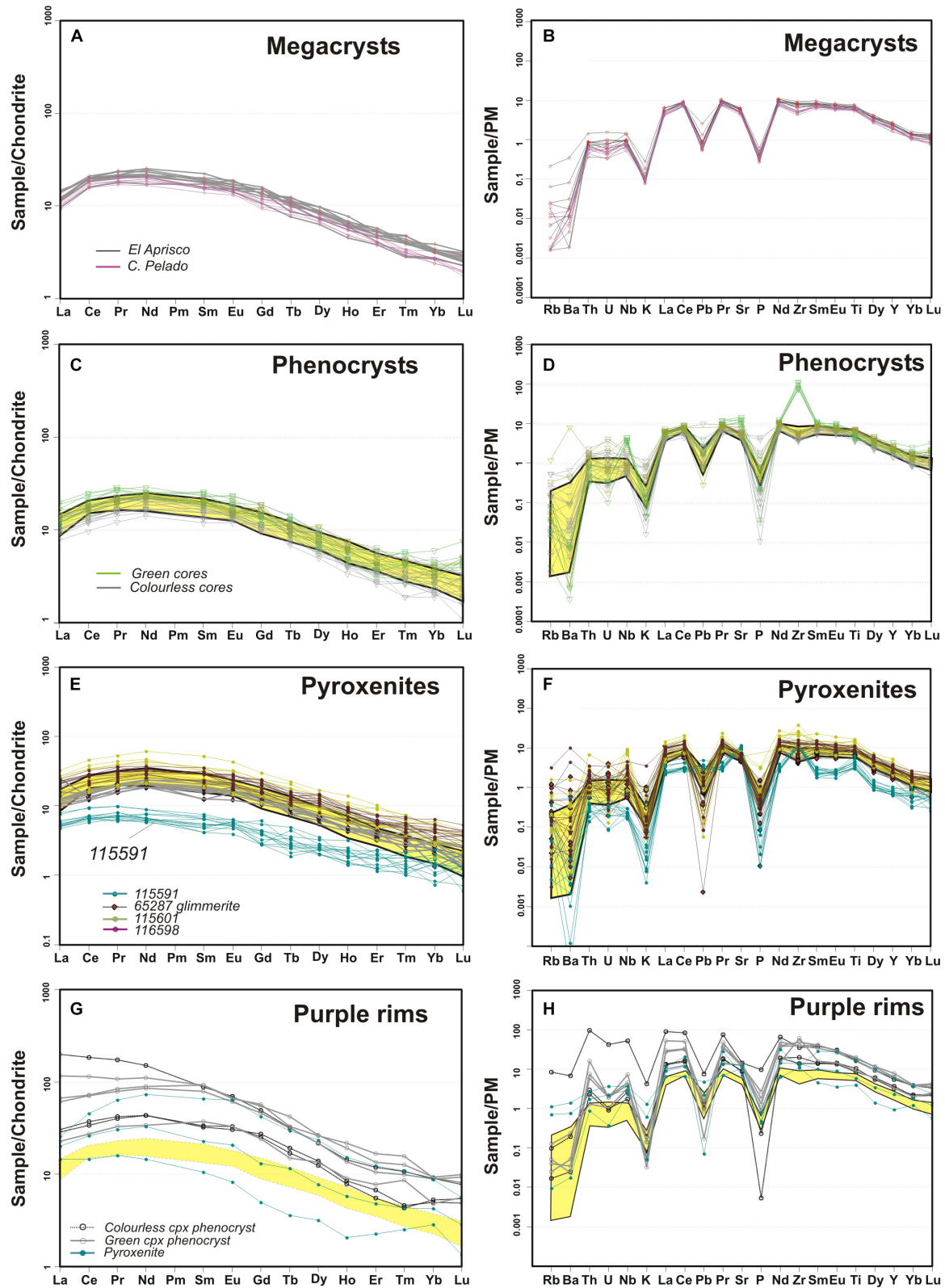
The phlogopite megacryst has very low (subchondritic) REE-Y contents (**Figure 8C**). Its LILE (K, Rb, Ba) and Cr-Ni-(Ti) contents are higher than those of amphibole, as can be seen in multitrace primitive mantle-normalized diagrams (**Figure 8D**). To our knowledge, there are no published trace element contents of phlogopite megacrysts from any Cenozoic volcano of the European Western circum-Mediterranean area, although this hydrous mafic mineral is an occasional megacryst in some of these volcanic centers (Hegner et al., 1995; Shaw and Eyzaguirre, 2000; Mayer et al., 2014). Only phlogopite megacryst of Cenozoic melilitites from the Ahaggar Swell (Algeria) has similar trace element patterns with slightly higher contents than the studied crystals (Kaczmarek et al., 2016). It is interesting to note that
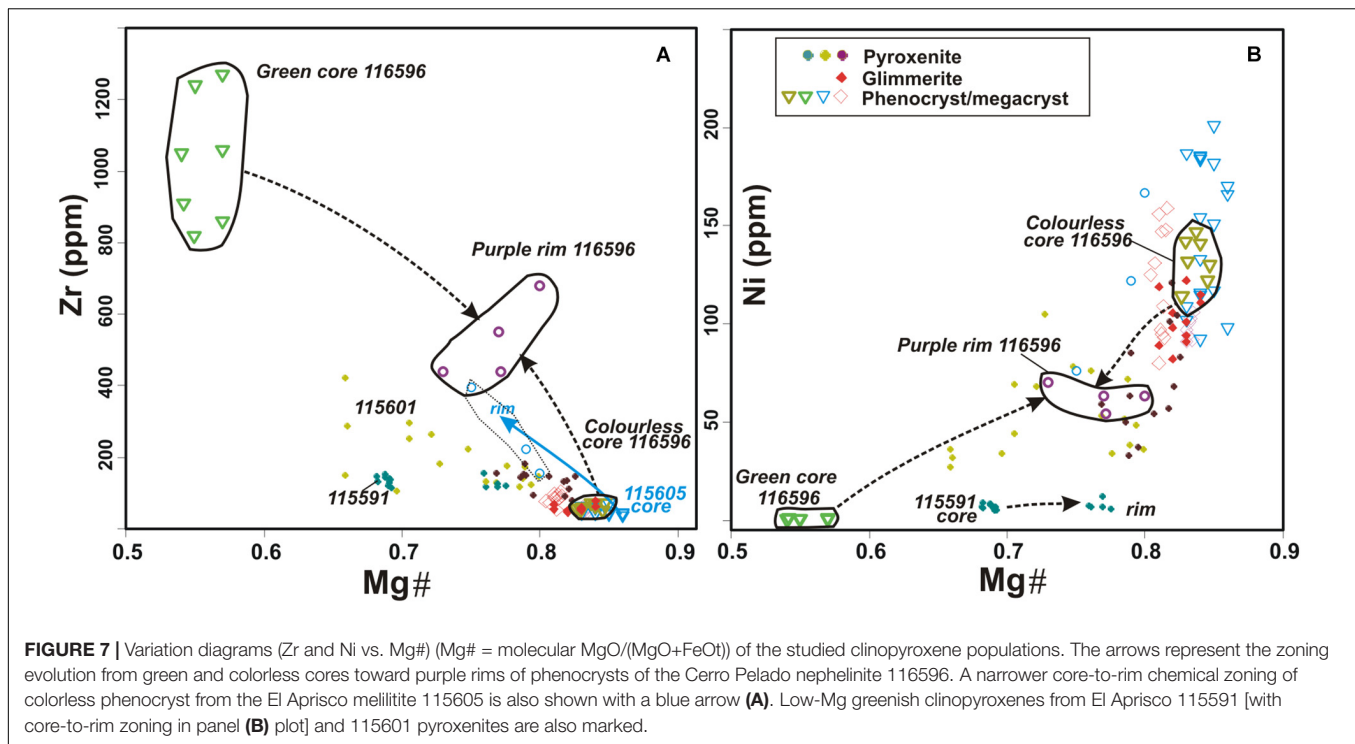
**FIGURE 6 |** REE and trace element composition of clinopyroxene: **(A)** and **(B)** megacrysts, **(C)** and **(D)** green and colorless phenocryst cores, **(E)** and **(F)** clinopyroxenite enclaves and **(G)** and **(H)** purple rims on colorless and green phenocryst cores and on clinopyroxene grains from pyroxenite enclaves. Chondrite-normalizing values are from Boynton (1985), whereas primitive mantle (PM) normalizing values are from Sun and McDonough (1989). The compositional field of clinopyroxene megacrysts (yellow field) is plotted in diagrams **(C–H)**.

**FIGURE 7 |** Variation diagrams (Zr and Ni vs. Mg#) (Mg# = molecular MgO/(MgO+FeOt)) of the studied clinopyroxene populations. The arrows represent the zoning evolution from green and colorless cores toward purple rims of phenocrysts of the Cerro Pelado nephelinite 116596. A narrower core-to-rim chemical zoning of colorless phenocryst from the El Aprisco melilitite 115605 is also shown with a blue arrow **(A)**. Low-Mg greenish clinopyroxenes from El Aprisco 115591 [with core-to-rim zoning in panel **(B)** plot] and 115601 pyroxenites are also marked.

from pyroxenite cumulates shows positive Zr (Hf) and Nb (Ta) anomalies in multi-trace element patterns (**Figure 6F**), although less marked than green phenocryst cores of sample 116596.

Amphiboles from the pyroxenite enclaves yield a more heterogeneous composition than megacrysts, although certain overlapping between both fields exists (**Figure 8**). Amphiboles from pyroxenite 115591 (El Aprisco) display the lowest Mg# values (up to 0.59), and something similar can be observed for REE, Y, Th, P and Ti (**Figures 8A,B**). On the contrary, amphiboles from this sample exhibit higher Pb and Zr (Hf) contents, similar to the accompanying greenish clinopyroxene, and consequently yield positive Pb and Zr (Hf) peaks in the multi-trace element pattern (**Figure 8B**).

The trace element composition of phlogopite is highly variable (**Supplementary Table S3**) reaching extreme values in the clinopyroxenite and glimmerite enclaves, whereas phlogopite megacrysts and phenocrysts show an intermediate composition within that broader range but display similar normalized trace element patterns (**Figures 8C,D**). The mica from the glimmerite enclave has Mg# values similar to megacrysts and phenocrysts (averaging 0.83) and the highest REE contents, in contrast to phlogopite from pyroxenite enclave 115601, which shows the lowest REE and Th-U contents and the lowest Mg# (averaging 0.71) of all the studied micas (**Figures 8C,D**).
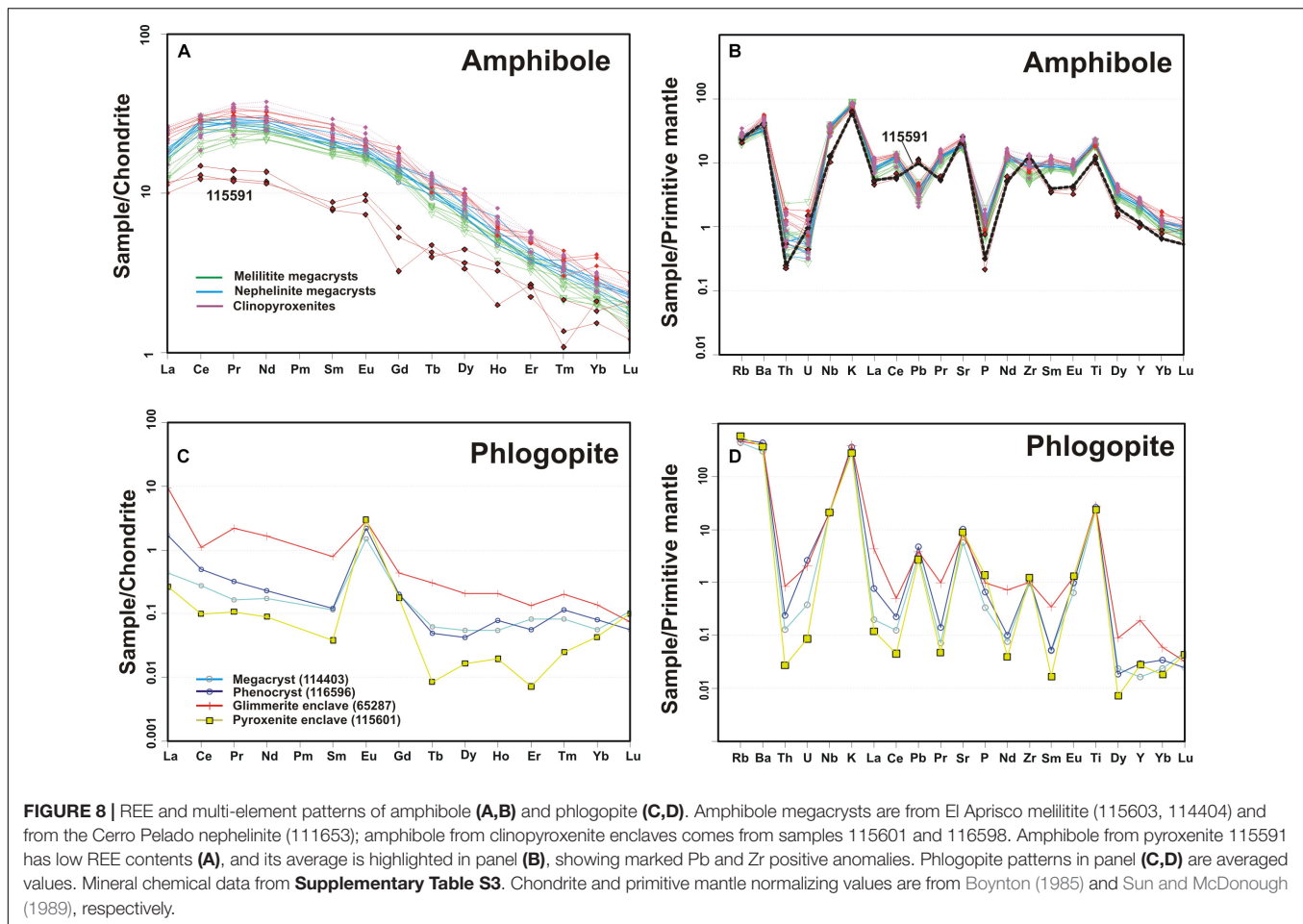
## DISCUSSION

### Origin of Megacrysts and Phenocrysts

It is not unusual that large mafic minerals (clinopyroxene, amphibole, phlogopite) were found within alkaline mafic to

ultramafic rocks. The origin of these megacrysts is controversial and could be either xenocrystic (i.e. mantle-derived) or phenocrystic/antecrystic (i.e. melt-derived). In the former case, megacrysts could be considered fragments of mantle wall-rocks, whereas melt-derived megacrysts could be either (i) pieces of mantellic cumulates unrelated to the host melt or (ii) minerals crystallized at high pressure conditions from their host volcanic magma or a cogenetic melt fraction (e.g. Shaw and Eyzaguirre, 2000; Gernon et al., 2016). The textural features and major element chemistry of the studied mafic megacryst-phenocrysts strongly support that the most primitive minerals were close to equilibrium and crystallized from primitive melts with a composition similar to that of the El Aprisco and Cerro Pelado volcanic rocks (Villaseca et al., 2019a). Nevertheless, the existence of different types of phenocryst cores with a variable composition, and the presence of reaction textures and mineral zoning indicates a more complex scenario.
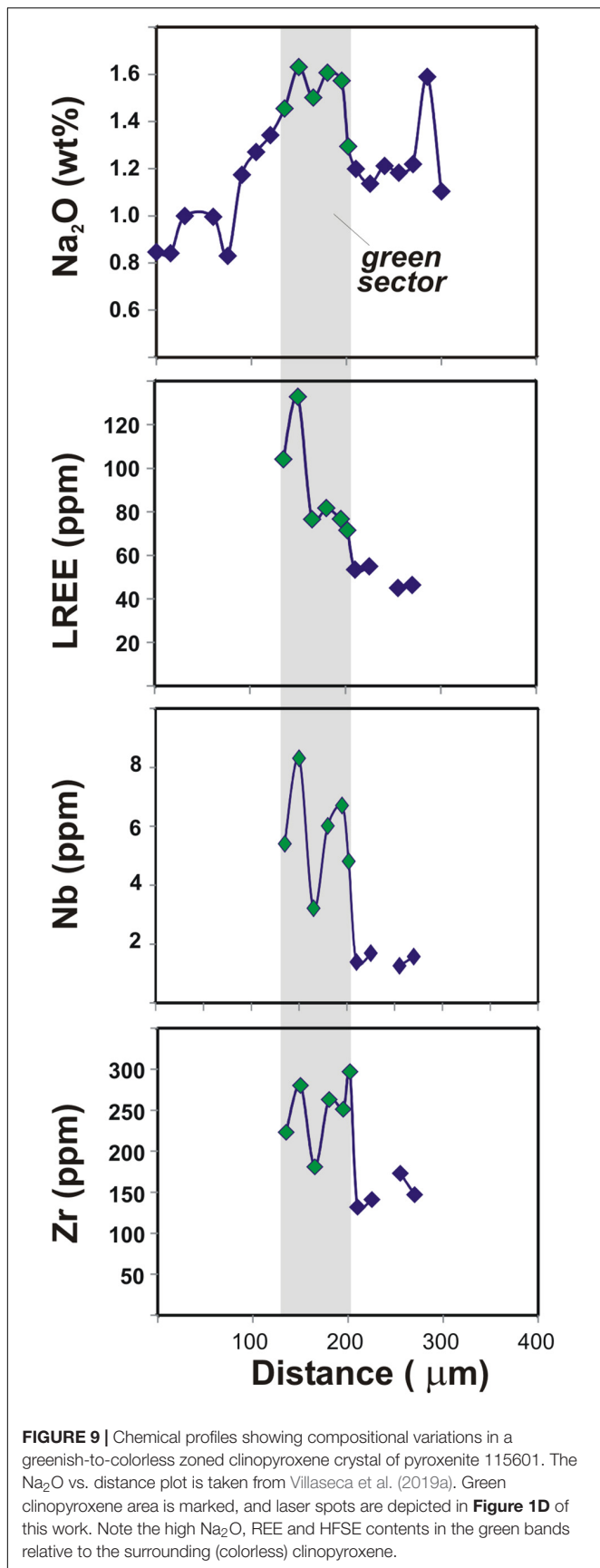
A xenocrystic origin of the megacrysts is not favored on the basis of several petrological and geochemical features. The crystal size (a few millimeters) and the interstitial character of the metasomatic hydrous phases in peridotites (amphibole and phlogopite) do not support the possibility of the large mafic crystals being fragments from these mantle rocks. The major element mineral composition is also different in the peridotites and the megacrysts and phenocryst cores: mainly, the lower Mg# and Cr and higher Ti values shown by the latter minerals (Villaseca et al., 2019a). Mineral trace element data reinforces this conclusion, since a clear disagreement exists between the geochemistry of the lherzolite minerals and that of megacrysts. These discrepancies are apparent for most elements in the El Aprisco volcano (clinopyroxene and amphibole composition;

**FIGURE 8 |** REE and multi-element patterns of amphibole **(A,B)** and phlogopite **(C,D)**. Amphibole megacrysts are from El Aprisco melilitite (115603, 114404) and from the Cerro Pelado nephelinite (111653); amphibole from clinopyroxenite enclaves comes from samples 115601 and 116598. Amphibole from pyroxenite 115591 has low REE contents **(A)**, and its average is highlighted in panel **(B)**, showing marked Pb and Zr positive anomalies. Phlogopite patterns in panel **(C,D)** are averaged values. Mineral chemical data from **Supplementary Table S3**. Chondrite and primitive mantle normalizing values are from Boynton (1985) and Sun and McDonough (1989), respectively.

**Figures 10C,D**, **11E,F**) and also for REE, Th, U, Nb and Ti of lherzolite clinopyroxene from the Cerro Pelado scoria cone (**Figures 10A,B**). Nevertheless, some similarities can be found for both major and trace elements only when comparing with the heterogeneous composition of clinopyroxene from wehrlite xenoliths from the Cerro Pelado volcano. However, this similitude is likely associated with the metasomatic origin of these wehrlites, since its metasomatic signature is genetically related to reaction with the host nephelinitic magma (Villaseca et al., 2010). Accordingly, the metasomatic amphibole and phlogopite of the Cerro Pelado wehrlite xenoliths display similar trace element patterns to those shown by the associated megacrysts, which are high-pressure fractionates derived from similar melts (**Figures 11A–D**). Nevertheless, this geochemical resemblance does not necessarily imply that megacrysts represent wehrlite fragments, which is not supported by petrographic features. Moreover, green clinopyroxene phenocryst cores have chemical features clearly different to wehrlitic clinopyroxene, including their notorious Zr positive peak in multitrace element patterns (**Figure 6**), also indicating a non-xenocrystic (mantle fragmentation) origin for these deep-seated crystals.

It has been long recognized that convex-upward REE patterns, such as those depicted by the Calatrava clinopyroxene and amphibole megacrysts, are typical of minerals crystallized from alkaline mafic magmas at high-pressure (Irving and Frey, 1984). Colorless clinopyroxene phenocryst cores display a chemical composition overlapping that of the equivalent megacrysts. This feature, which has also been observed for the major elements (Villaseca et al., 2019a), is apparent for the trace elements (**Figures 6C,D**) and implies that they all must share a common origin as deep mineral fractionates. Studied clinopyroxene and amphibole megacrysts are in chemical equilibrium, as their intermineral partition coefficients (see comments above) are close to those previously published for basic-ultrabasic lithotypes (Vannucci et al., 1995; Raffone et al., 2009). This suggests that they are cogenetic phases derived from the same magma. This is confirmed by the similar composition of the liquids in equilibrium with studied clinopyroxene and amphibole calculated using mineral/melt distribution coefficients of high-$T$ and high-$P$ basaltic systems (Hart and Dunn, 1993; La Tourrette et al., 1995; Ionov et al., 1997; **Figure 12**). The results compare well with the whole-rock data of the Calatrava host magmas, with REE patterns of similar slope and equivalent positive and negative trace element anomalies (**Figure 12**). Nevertheless, the higher chemical heterogeneity shown by the calculated melts with megacryst/phenocryst clinopyroxene, mainly for the LIL

**FIGURE 9 |** Chemical profiles showing compositional variations in a greenish-to-colorless zoned clinopyroxene crystal of pyroxenite 115601. The Na₂O vs. distance plot is taken from Villaseca et al. (2019a). Green clinopyroxene area is marked, and laser spots are depicted in **Figure 1D** of this work. Note the high Na₂O, REE and HFSE contents in the green bands relative to the surrounding (colorless) clinopyroxene.

elements (Rb, Ba, Th, U), is likely associated with the variable composition of these mafic minerals and the evolution of magma at deep stagnation levels. Even so, the broad similarity between the calculated melts and the Calatrava volcanics indicates that mafic megacrysts derive from high-pressure fractional crystallization of melts with a composition similar to that of the host alkaline magmas.

On the other hand, the Fe-rich green clinopyroxene phenocryst cores are slightly trace element-enriched (remarkably for Zr), and some purple clinopyroxene rims are clearly different from other clinopyroxenes due to their elevated trace element concentrations (**Figures 6G,H**). The calculated geochemical heterogeneity of equilibrated melts with these clinopyroxene types (**Figures 12A–D**) supports the involvement of magmas with a variable degree of evolution for their origin, within a complex scenario of crystallization at different levels in the upper lithosphere (see discussion below).
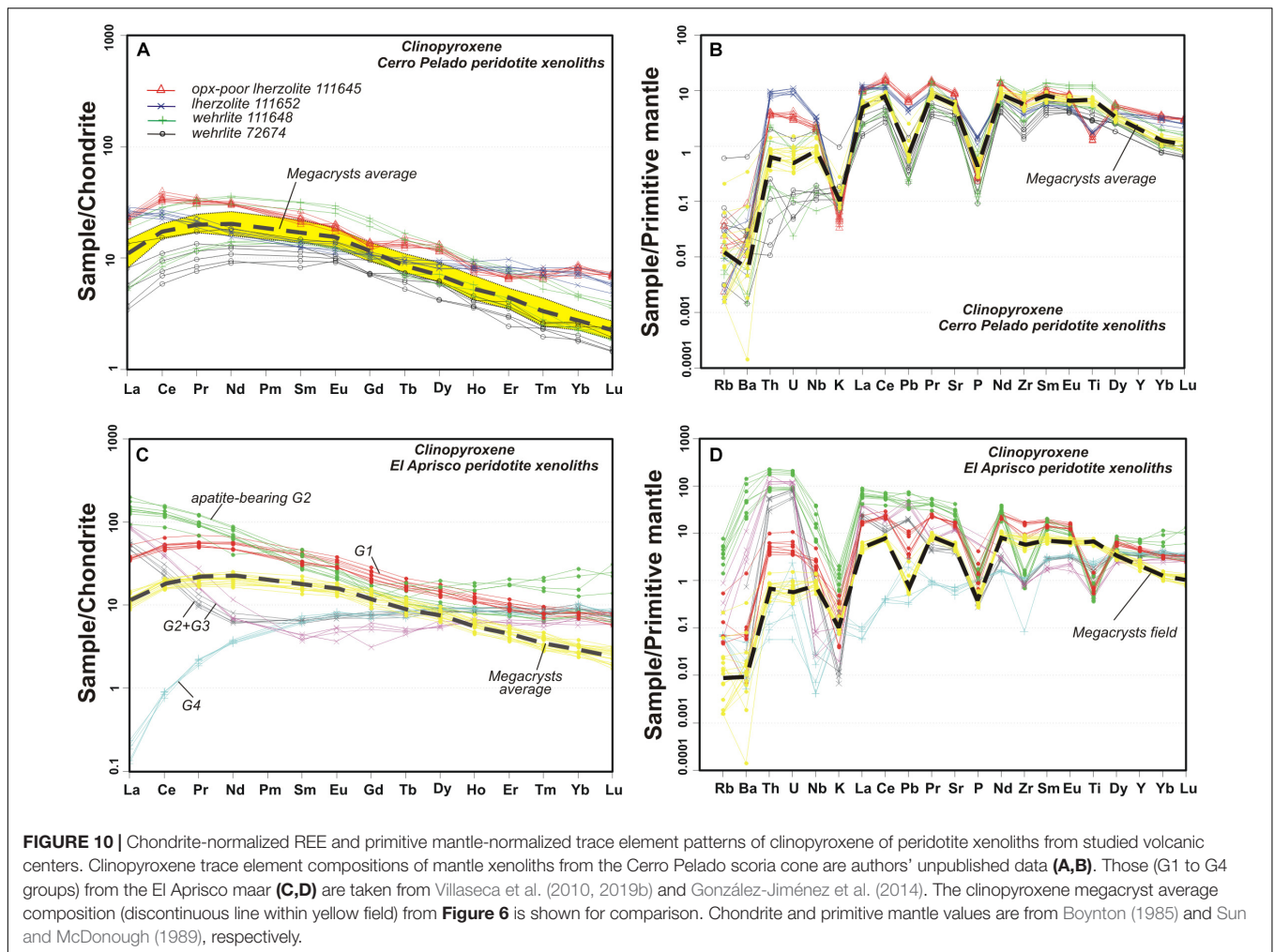
## Origin of Pyroxenite and Glimmerite Enclaves

The Calatrava clinopyroxenite and glimmerite enclaves do not have characteristics of xenolithic mantle rocks. While minerals in peridotites and metasomatic veins are usually unzoned and very homogeneous in major element composition (Villaseca et al., 2010; Lustrino et al., 2016), clinopyroxene and amphibole of the studied pyroxenites display oscillatory or patchy zoning, (respectively), commonly interpreted as igneous textures. The absence of exsolution lamellae in clinopyroxene from these enclaves also contradicts their origin as wall-rock mantle fragments entrapped by the ascending basic magma (Villaseca et al., 2019a).

The mineral geochemistry also favors the magmatic origin of the Calatrava pyroxenite and glimmerite enclaves, due to their low Mg# values when compared to those of the mantle minerals (<0.85; Villaseca et al., 2019a). The trace element composition of the main mafic minerals of these enclaves (colorless clinopyroxene, amphibole and phlogopite) is coincident with that of the megacrysts and colorless phenocryst cores dispersed within the host volcanic magma (**Figures 6, 8**), which implies that they crystallized from similar cogenetic basic melts. Nevertheless, liquids in equilibrium with greenish clinopyroxene from these enclaves show REE patterns parallel to those from the Calatrava volcanics but showing different REE contents (**Figure 12C**) or having spikier trace element patterns with a marked Zr positive anomaly that is absent in Calatrava volcanic rocks (**Figure 12D**), as was the case with the data from green clinopyroxene phenocryst cores.

## Relationships Between Magmatism and Metasomatism Within Peridotite Wall-Rocks

As shown above, we have observed similarities among the trace element compositions of clinopyroxene, amphibole and phlogopite megacrysts in the Cerro Pelado center and the equivalent metasomatic phases in associated peridotite xenoliths, mostly in the case of the "Fe-Ti metasomatised" wehrlites. These
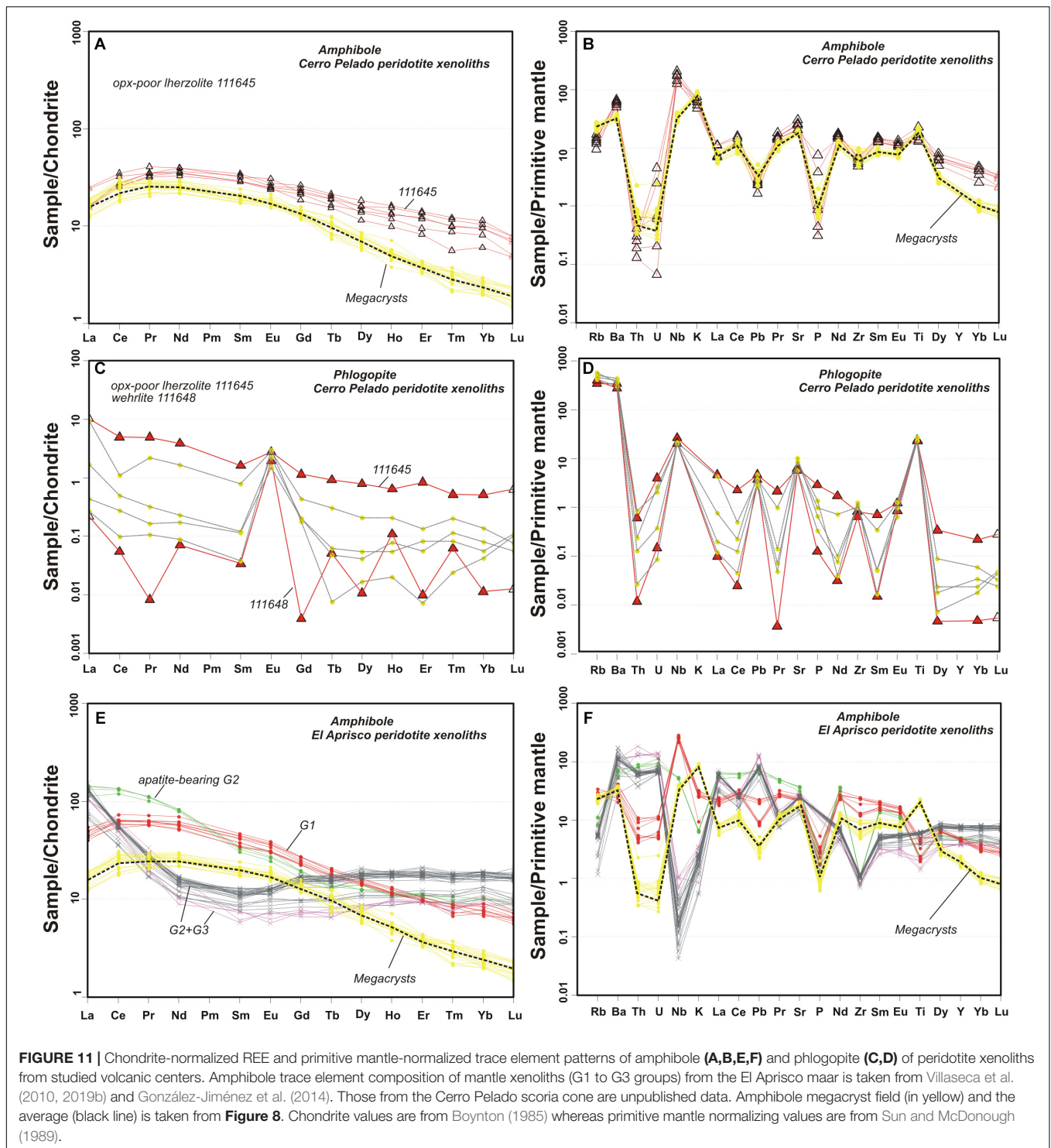
**FIGURE 10 |** Chondrite-normalized REE and primitive mantle-normalized trace element patterns of clinopyroxene of peridotite xenoliths from studied volcanic centers. Clinopyroxene trace element compositions of mantle xenoliths from the Cerro Pelado scoria cone are authors' unpublished data **(A,B)**. Those (G1 to G4 groups) from the El Aprisco maar **(C,D)** are taken from Villaseca et al. (2010, 2019b) and González-Jiménez et al. (2014). The clinopyroxene megacryst average composition (discontinuous line within yellow field) from **Figure 6** is shown for comparison. Chondrite and primitive mantle values are from Boynton (1985) and Sun and McDonough (1989), respectively.

latter enclaves have neoblastic spongy clinopyroxene (samples 72674 and 116648) and interstitial phlogopite, amphibole and alkaline glass. Taking into account that the studied megacrysts-phenocrysts crystallized from magmas similar in composition to their present host melts, the compositional similarities might indicate that the metasomatic agents which reacted with the Cerro Pelado peridotites and the host alkaline mafic magmas were genetically related. In fact, previous studies in those mantle xenoliths already established that they had undergone mafic silicate metasomatism, and that the most metasomatised wehrlites were probably connected with reactive infiltration of alkaline melts similar to their host magmas (Villaseca et al., 2010). Thus, although some interstitial amphibole and phlogopite in lherzolites record reaction with the Calatrava alkaline magma, these hydrous minerals would rarely give rise to euhedral cm-sized megacrysts, and their much higher Mg and Cr contents make it easy to discriminate magmatic megacrysts of melt-mantle metasomatic minerals from strongly transformed mantle xenoliths (Yu et al., 2019). Neither amphibole- (or phlogopite-) rich pegmatite-like veins nor large idiomorphic crystals (megacrysts) have been recorded in the studied peridotite suites.

Mantle xenoliths from the El Aprisco maar have metasomatic phases remarkably different in composition to the studied megacrysts and phenocrysts. The study of these mantle xenoliths has enabled the identification of at least three old metasomatic events occurring during the Cretaceous (~118 Ma), the Oligocene (~29 Ma) and the Miocene (~16–4 Ma) (Villaseca et al., 2019b). As in the case of the Cerro Pelado peridotites, the high Cr, Ni and Sc contents of metasomatic amphiboles from the El Aprisco peridotite suites also agree with a longer time of equilibration within the mantle in comparison to the much younger age of mafic minerals formed during the Calatrava volcanic event (2.8 to 2.2 Ma ages for megacrysts formed in both volcanic centers, after Villaseca et al., 2019b), even if their formation occurred at similar *P-T* conditions at mantle depths.
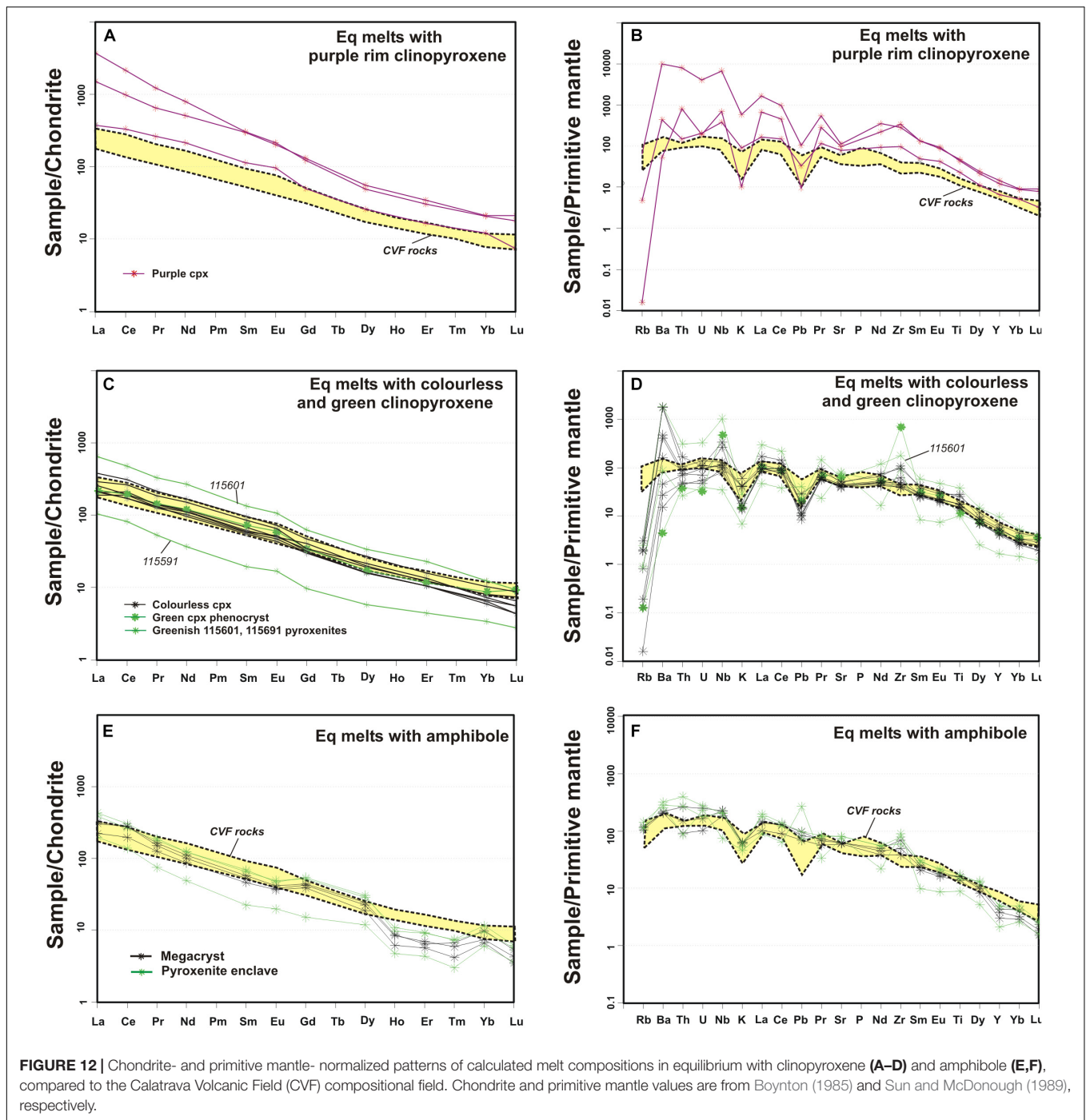
## Melting, Storage and Melt Evolution Within a Magmatic Plumbing System

The main alkaline silica-undersaturated magmas of the Calatrava Volcanic Field have been interpreted as being generated from a mantle asthenosphere source with trace element and isotopic ratios similar to the HIMU (or EAR) OIB-reservoir

**FIGURE 11 |** Chondrite-normalized REE and primitive mantle-normalized trace element patterns of amphibole **(A,B,E,F)** and phlogopite **(C,D)** of peridotite xenoliths from studied volcanic centers. Amphibole trace element composition of mantle xenoliths (G1 to G3 groups) from the El Aprisco maar is taken from Villaseca et al. (2010, 2019b) and González-Jiménez et al. (2014). Those from the Cerro Pelado scoria cone are unpublished data. Amphibole megacryst field (in yellow) and the average (black line) is taken from **Figure 8**. Chondrite values are from Boynton (1985) whereas primitive mantle normalizing values are from Sun and McDonough (1989).

(Cebriá and López Ruiz, 1995). Phlogopite and garnet are considered residual phases in the mantle sources, consistent with the fractionated HREE patterns and negative K anomalies shown by Calatrava volcanic rocks (**Figure 4**). The determination of accurate *P-T* conditions of mantle melting is challenging. We have considered the geothermobarometry approach of Lee

et al. (2009), which estimates the *P-T* condition of basaltic melt extraction in equilibrium with an averaged lherzolitic peridotite source. The high MgO content (>10 wt%) of most of the Calatrava magmas (**Table 1**) renders them suitable for this calculation. Nevertheless, some studied rocks have no features of primary melts. Thus, samples with MgO > 18 wt% and

**FIGURE 12 |** Chondrite- and primitive mantle- normalized patterns of calculated melt compositions in equilibrium with clinopyroxene **(A–D)** and amphibole **(E,F)**, compared to the Calatrava Volcanic Field (CVF) compositional field. Chondrite and primitive mantle values are from Boynton (1985) and Sun and McDonough (1989), respectively.

pyroxenite enclaves have been excluded due to their high crystal cargo or cumulate origin, respectively. The resulting pressure and temperature of melt segregation from the mantle source are in the range of 2.3 to 5.6 GPa and 1,300 to 1,540°C, respectively (**Table 1**). These values have to be considered as rough estimates of partial melting conditions for Calatrava magmas from a lherzolite protolith. It is interesting to note that these estimations imply melt extraction within the stability field of garnet, in agreement with the chemical features of these alkaline magmas.

During their ascent, some of the Calatrava magmas were arrested in shallow lithospheric mantle reservoirs, where fractional crystallization was triggered. This is illustrated by the formation of a suite of mafic megacryst-phenocrysts and pyroxenitic cumulates, such as those described in this study. The conditions of crystallization indicate pressures of 1.2–1.6 GPa and temperatures in the range 1,275–1,350°C, corresponding to the uppermost mantle (Villaseca et al., 2019a). The relative wide depth range for magma stagnation derived from the pressure

data could imply either a polybaric crystallization during melt ascent or uncertainties in the *P-T* calculations. In any case, the much lower pressure provided by clinopyroxene phenocryst purple rims (~0.3–0.8 GPa, Villaseca et al., 2019a) points to the formation of these overgrowths during the magma transport through the crust.

The presence of clinopyroxene phenocrysts of contrasted composition (colorless and green cores), sharing similar purple rims, reveals a complex magmatic story. The green cores are enriched in Fe and incompatible trace elements when compared to the colorless cores, and the corresponding melts in equilibrium must represent a more evolved composition (**Figure 13**). This feature is indicative of a magma differentiation process occurring at depth and responsible for the formation of a heterogeneous suite of mafic minerals with a variable degree of evolution. Clinopyroxene and amphibole might be the main liquidus minerals during magma crystallization at depth due to their modal abundance as megacrysts and mineral phases in pyroxenite enclaves. Phlogopite and olivine (and accessory Fe-Ti-rich minerals) were also involved in minor proportions. As an approximation of this process, we have applied a model of fractional crystallization starting from a melt $C_0$ representing a primitive host basaltic composition (see caption to **Figure 13**) and assuming clinopyroxene + amphibole + minor olivine

fractionation. The distribution coefficients used are those of La Tourrette et al. (1995) (Zr-Hf) and Irving and Frey (1984) (REE) for amphibole; Hart and Dunn (1993) for clinopyroxene and Adam and Green (2006) for olivine. The results indicate that a high degree of fractionation is needed (up to 80%) in order to obtain the high Zr/Hf and the slightly low Gd/Yb ratios of the evolved melts equilibrated with green clinopyroxene (**Figure 13**). The presence of mica-rich (glimmerite) enclaves is an evidence in favor of phlogopite crystallization during differentiation, but its participation does not change significantly the above estimated evolution pattern.

A fractional crystallization process also explains the clinopyroxene zoning in pyroxenite enclaves, with variable Mg# (around 0.65 in the green bands and 0.82 in the colorless core) and trace element contents within the same crystal (**Figure 9**). The fact that this zoning is frequently oscillatory requires a connection with a more primitive magma batch acting as a recharge source. The geochemical similarities shared by the evolved green phenocrysts cores and the pale green clinopyroxenes in pyroxenites supports their formation in a similar context: magma pools stagnated within the mantle. We think that magmas slightly more primitive than the volcanic host melts evolved by fractional crystallization within mantle reservoirs, generating a wide range of liquid compositions (either more primitive or significantly more fractionated) at local scale. This large chemical heterogeneity contrasts with the coincident isotopic composition of megacrysts, pyroxenite enclaves and host rocks (**Figure 5**), which is indicative of the cogenetic nature of the involved magmas. This model contrast with previous works studying clinopyroxene green phenocryst cores in alkaline volcanoes of the European circum-Mediterranean region, where their origin from significantly more evolved melts than host lavas was interpreted as xenocrystic fragments from non-cogenetic rocks (Aulinas et al., 2013; Jankovics et al., 2013; Matusiak-Malek et al., 2018).

A typical feature of chilled margins in cooling magmatic bodies is the presence of interstitial highly fractionated liquids within crystal mush carapaces (e.g. Marsh, 1996). The pyroxenitic cumulates found in the Calatrava volcanic rocks can be considered pieces of this crystalline margin, and the complex zoned crystals they include serve as evidence of the involvement of highly evolved melts. These latter liquids could give rise to single microcrysts (green phenocryst cores), subsequently incorporated as crystal cargo in ascending and less fractionated magmas from the same magmatic system. Nevertheless, there are several differences between the trace element composition of melts in equilibrium with green clinopyroxene and the most evolved Calatrava volcanic rocks, such as the marked Zr content of green phenocryst cores (**Figures 12**, **13**). The highly evolved liquids which gave rise to the low-Mg green clinopyroxene have not been erupted in Calatrava volcanoes, and were probably trapped within the cumulate chilled margins of deep mantle reservoirs. The small volume of highly fractionated liquids generated hinders to collect them to be transported toward the Earth's surface; they are relatively immobile.



**FIGURE 13 |** Gd/Yb vs Zr/Hf ratios of melts equilibrated with clinopyroxenes. The compositional field of Calatrava Volcanic Field (CVF) magmas is also shown for comparison. The clinopyroxene compositions used for calculations are averaged values for selected colorless megacrysts (115603, 114404, 111639) and phenocryst cores (115605, 116596), together with green phenocryst cores (116596) and pyroxenites (115601, 115591). Purple rims overgrow phenocrysts (115605, 116596) and pyroxenite crystals (115591) (see **Supplementary Table S2** for averaged clinopyroxene values). The $C_0$ for the fractional crystallization model is the CAL-73 nephelinite (from the Cerro Pelado volcano, CP in figure). The arrow represents the trend of chemical evolution of melts based on the fractionation model (up to 80% of fractional crystallization) considering extraction of 45% clinopyroxene + 45% amphibole + 10% olivine.

The major and trace element composition of the clinopyroxene purple rims is broadly intermediate between primitive colorless and evolved green cores (**Figures 8**, **13**; see also Villaseca et al., 2019a). Purple rims can be found overgrowing both types of phenocryst cores and also forming the most external margin of clinopyroxene in some marginal areas of pyroxenite enclaves. It is thus likely that rims were formed from the magma that entrapped megacrysts, phenocrysts and enclaves, and erupted at the Earth's surface. This conclusion is supported by the broadly similar composition of calculated melts in equilibrium with thin purple rims and the host melts (**Figure 13**). Other rims provide equilibrated melts with trace element contents significantly higher than the Calatrava magmas (**Figures 12**, **13**). This feature is in accordance with an increase in the cooling and decompression rates, during the rise of magma toward the surface, which favors the enrichment in incompatible trace elements as a consequence of modification of the partitioning of elements and crystallization being governed by kinetic effects (e.g. Re et al., 2017 and references therein).

The crystal fractionation process described in this study adds novel information regarding the magmatic differentiation associated with deep plumbing systems beneath monogenetic volcanos. Mafic mineral crystallization is one of the main factors controlling magma differentiation inducing changes in magma buoyancy, volatile composition and, eventually, the onset of volcanic eruption (Mattsson et al., 2013; Re et al., 2017). The cumulate origin of clinopyroxene, amphibole and phlogopite, assessed via trace element modeling, implies that the primary magmas were volatile-rich and that a significant proportion of minerals was removed from the melt due to crystal fractionation at mantle reservoirs. It is commonly accepted that volcanic eruptions of carbonate-rich nephelinitic and melilititic magmas generating large maar-diatreme volcanoes can be triggered by pressure oversaturation associated with deep exsolution of $CO_2$ due to silicate crystallization (e.g. Mattsson et al., 2013). This process is favored by decompression during magma ascent or due to recharge of deep juvenile volatile-rich melts into the magma reservoirs (Ubide et al., 2019 and references therein). Although such discussion is beyond the scope of this work, our data leaves open the possibility of the $CO_2$ increase being related with deep-seated crystal fractionation (Villaseca et al., 2019a). The combination of $CO_2$ increase in the environs of the solidification front and upward movement of magma within the upper mantle could explain magma boiling, fragmentation and a rapid ascent to the surface, carrying a heterogeneous suite of crystals, pyroxenitic enclaves and mantle xenoliths.

## CONCLUSION

This is the first study focused on the characterisation and interpretation of the trace element mineral chemistry of phenocrysts, megacrysts, and clinopyroxenite and glimmerite enclaves carried by alkaline rocks of the Calatrava volcanic field (El Aprisco and Cerro Pelado volcanoes), central Spain. Mineral data were complemented with whole-rock and isotopic (Sr-Nd)

data of megacrysts, enclaves and volcanic rocks. Mineral analyses focused on clinopyroxene, amphibole and phlogopite, which appear as megacrysts and phenocrysts, and as main constituents of the pyroxenite enclaves. The mafic megacrysts display a chemical composition more akin to an origin as deep segregates rather than fragments of a peridotitic mantle. They show clear differences in composition when compared to minerals from the mantle xenoliths carried by the Calatrava volcanics but are similar to the same phases in clinopyroxenite and glimmerite enclaves.

The presence of disequilibrium textures, complex zoning and contrasting compositions in clinopyroxene crystals indicates that they did not crystallize from a single melt. Clinopyroxene is the most common and widespread phase, occurring as megacrysts, macrocrysts and phenocrysts in these volcanic rocks. Two types of high-P crystals of different colors have been observed: green and colorless phenocryst cores. The former are less abundant and have low Mg# (Cr, Ni, Sc) and high Zr-Sr contents, which is indicative of their derivation from melts much more fractionated than those related to the primitive high Mg# colorless cores. The contrasting compositions also coexists in complexly zoned crystals of clinopyroxenites, suggesting that the colorless and green types might be cognate and derive from mixing of primitive and evolved fractionated liquids within the same magmatic system. The geochemistry of clinopyroxene supports a fractionation process mainly controlled by clinopyroxene and amphibole crystallization.

The similarity in mineral chemistry and the homogeneous whole-rock Sr-Nd ratios of all the analyzed minerals and rocks suggest that the deep fractionating magma batches and the melts transporting this complex crystal cargo were likely generated from similar sources. The possibility that this suite of fractionated magmas derive from a single magma batch is supported by the overlapping composition of the melts in equilibrium with the mafic megacrysts/phenocrysts and the volcanic host magmas and also may explain the presence of oscillatory zoning at micron-scale in some cumulates, linked to crystallization fronts in deep magma chambers, where repeated infiltration of recharging external liquids is probably limited. This model contrasts with previous studies that suggested that clinopyroxene green phenocryst cores in alkaline melts are xenocrystic fragments from non-cogenetic rocks.

## DATA AVAILABILITY STATEMENT

All datasets generated for this study are included in the article/**Supplementary Material**.

## AUTHOR CONTRIBUTIONS

All authors collaborated in the sampling, petrographic study and the performing of analytical data and contributed to the final version of the manuscript, figures, and tables. CV conceived the study and wrote an original draft later improved with inputs from JG and DO.

# FUNDING

# ACKNOWLEDGMENTS

# SUPPLEMENTARY MATERIAL

The Supplementary Material for this article can be found online at: https://www.frontiersin.org/articles/10.3389/feart.2020.00132/full#supplementary-material

**FIGURE S1 | (A)** The Calatrava Volcanic Field and location of the two studied volcanoes: El Aprisco and Cerro Pelado (Ancochea, 1982; Cebriá et al., 2011). **(B)** Sketch map of the Iberian Peninsula showing the location of the main Cenozoic volcanic fields (in black; Lustrino and Wilson, 2007).

**TABLE S1 |** Compositional data on certified standards analyzed with the samples in this study.

**TABLE S2 |** Clinopyroxene trace element contents (in ppm) in megacrysts, phenocrysts and pyroxenite enclaves.

**TABLE S3 |** Amphibole and phlogopite trace element contents (in ppm) in megacrysts, phenocrysts and pyroxenite enclaves.

# REFERENCES

Adam, J., and Green, T. (2006). Trace element between mica- and amphibole-bearing garnet lherzolite and hydrous basanitic melt: 1. Experimental results and the investigation of controls on partitioning behavior. *Contrib. Mineral. Petrol.* 152, 1–17.

Allègre, C. J., and Turcotte, D. L. (1986). Implications of a two-component marble-cake mantle. *Nature* 323, 123–127.

Ancochea, E. (1982). *Evolución Espacial y Temporal del Volcanismo Reciente de España Central.* Ph.D. thesis., Universidad Complutense de Madrid, Madrid.

Aulinas, M., Gisbert, G., Gimeno, D., and Gasperini, D. (2013). Cannibalization of previous Na-rich clinopyroxenes by ascending magmas of the Garrotxa Volcanic Field (NE, Spain). *Mineral. Mag.* 77:631.

Bodinier, J. L., Guiraud, M., Fabries, J., Dostal, J., and Dupuy, C. (1987). Petrogenesis of layered pyroxenites from the Lherz, Freychinede and Prades ultramafic bodies (Ariege, French Pyrenees). *Geochim. Cosmochim. Acta* 51, 279–290.

Boynton, W. V. (1985). "Geochemistry of the rare earth elements: meteorite studies," in *Rare Earth Element Geochemistry*, ed. P. Henderson (New York, NY: Elsevier), 63–114. doi: 10.1186/s12932-015-0022-4

Cebriá, J. M. (1992). *Geoquímica de las Rocas Basálticas y Leucititas de la Región Volcánica de Campo de Calatrava, España.* Ph.D. thesis., Universidad Complutense de Madrid, Madrid.

Cebriá, J. M., and López Ruiz, J. (1995). Alkali basalts and leucitites in an extensional intracontinental plate setting: the late Cenozoic Calatrava volcanic province (central Spain). *Lithos* 35, 27–46.

Cebriá, J. M., Martín-Escorza, C., López-Ruiz, J., Morán-Zenteno, D. J., and Martiny, B. M. (2011). Numerical recognition of alignments in monogenetic volcanic areas: examples from the Michoacán-Guanajato Volcanic Field in Mexico and Calatrava in Spain. *J. Volcan. Geotherm. Research* 201, 73–82. doi: 10.1016/j.jvolgeores.2010.07.016

Chazot, G., Menzies, M. A., and Harte, B. (1996). Determination of partition coefficients between apatite, clinopyroxene, amphibole, and melt in natural spinel lherzolites from Yemen: implications for wet melting of the lithospheric mantle. *Geochim. Cosmochim. Acta* 60, 423–437.

Downes, H. (2007). Origin and significance of spinel and garnet pyroxenites in the shallow lithospheric mantle: ultramafic massifs in orogenic belts in Western Europe and NW Africa. *Lithos* 99, 1–24.

Downes, H., Reichow, M. K., Mason, P. R. D., Beard, A. D., and Thirlwall, M. F. (2003). Mantle domains in the lithosphere beneath the French Massif Central: trace element and isotopic evidence from mantle clinopyroxenes. *Chem. Geol.* 200, 71–87.

Duda, A., and Schmincke, H.-S. (1985). Polybaric differentiation of alkali basaltic magmas: evidences from green-core clinopyroxenes (Eifel, FRG). *Contrib. Mineral. Petrol.* 91, 340–353.

Garrido, C. J., and Bodinier, J. L. (1999). Diversity of mafic rocks in the Ronda Peridotite; evidence for pervasive melt–rock reaction during heating subcontinental lithosphere by upwelling asthenosphere. *J. Petrol.* 40, 729–754.

Gernon, T. M., Upton, B. G. J., Ugra, R., Yücel, C., Taylor, R. N., and Elliott, H. (2016). Complex subvolcanic magma plumbing system of an alkali basaltic maar-diatreme volcano (Elie Ness, Fife, Scotland). *Lithos* 264, 70–85.

González-Jiménez, J. M., Villaseca, C., Griffin, W. I., O'Reilly, S. Y., Belousova, E., Ancochea, et al. (2014). Significance of ancient sulfide PGE and Re-Os signatures in the mantle beneath Calatrava, Central Spain. *Contrib. Mineral. Petrol.* 168:1047.

Granet, M., Wilson, M., and Achauer, U. (1995). Imaging a mantle plume beneath the French Massif Central. *Earth Planet. Sci. Lett.* 136, 281–296.

Green, D. H., and Ringwood, A. E. (1964). Fractionation of basalt magmas at high pressures. *Nature* 201, 1276–1279.

Grégoire, M., Moine, B. N., O'Reilly, S. Y., Cottin, J. Y., and Giret, A. (2000). Trace element residence and partitioning in mantle xenoliths metasomatized by high alkaline silicate and carbonate-rich melts (Kerguelen Islands, Indian Ocean). *J. Petrol.* 41, 477–509.

Hart, S. R., and Dunn, T. (1993). Experimental cpx/melt partitioning of 24 trace element. *Contrib. Mineral. Petrol.* 113, 1–8.

Hegner, E., Walter, H. J., and Satir, M. (1995). Pb-Sr-Nd isotopic composition and trace element geochemistry of megacrysts and melilitites from the Tertiary Urach volcanic field: source composition of small volume melts under SW Germany. *Contrib. Mineral. Petrol.* 122, 322–335.

Ionov, D. A., Griffin, W. L., and O'Reilly, S. Y. (1997). Volatile-bearing minerals and lithophile trace elements in the upper mantle. *Chem. Geol.* 141, 153–184.

Irving, A. J., and Frey, F. A. (1984). Trace element abundances in megacrysts and their host basalts; constraints on partition coefficients and megacryst genesis. *Geochim. Cosmochim. Acta* 48, 1201–1221.

Jankovics, M. E., Dobosi, G., Embey-Isztin, A., Kiss, B., Sági, B., Harangi, S., et al. (2013). Origin and ascent history of unusually crystal-rich alkaline basaltic magmas from the western Pannonian Basin. *Bull. Volcanol.* 75:23.

Jankovics, M. E., Taracsák, Z., Dobosi, G., Embey-Isztin, A., Batki, A., Harangi, S., et al. (2016). Clinopyroxene with diverse origins in alkaline basalts from the western Pannonian Basin: implications from trace element characteristics. *Lithos* 262, 120–134.

Kaczmarek, M. A., Bodinier, J. L., Bosch, D., Tommasi, A., Dautria, J. M., and Kechid, S. A. (2016). Metasomatized mantle xenoliths as a record of the lithospheric mantle evolution of the northern edge of the Ahaggar Swell, In Teria (Algeria). *J. Petrol.* 57, 345–382.

Keenan, B., Huertas, M. J., and Ancochea, E. (2019). Edad y composición del volcán Bienvenida (Campos de Calatrava). *Geogaceta* 65, 23–26.

La Tourrette, T., Hervig, R. L., and Holloway, J. R. (1995). Trace element partitioning between amphibole, phlogopite, and basanite melt. *Earth Planet. Sci. Lett.* 135, 13–30.

Le Bas, M. J. (1989). Nephelinitic and basanitic rocks. *J. Petrol.* 30, 1299–1312.

Le Maitre, R. W. (ed.) (2002). *Igneous Rocks: A Classification and Glossary of Terms*. Cambridge: Cambridge University Press.

Lee, C. T. A., Luffi, P., Plank, T., Dalton, H., and Leeman, W. P. (2009). Constraints on the depths and temperatures of basaltic magma generation on Earth and other terrestrial planets using new thermobarometers for mafic magmas. *Earth Planet. Sci. Lett.* 279, 20–33.

Lierenfeld, M. B., and Mattsson, H. B. (2015). Geochemistry and eruptive behaviour of the Finca la Nava maar volcano (Campo de Calatrava, south-central Spain). *Int. J. Earth Sci.* 104, 1795–1817.

Liotard, J. M., Briot, D., and Boivin, P. (1988). Petrological and geochemical relationships between pyroxene megacrysts and associated alkali-basalts from Massif Central (France). *Contrib. Mineral. Petrol.* 98, 81–90.

Lustrino, M., Prelevic, D., Agostini, S., Gaeta, M., Di Rocco, T., Stagno, V., et al. (2016). Ca-rich carbonates associated with ultrabasic-ultramafic melts: carbonatite or limestone xenoliths? A case study from the late Miocene Morron de Villamayor volcano (Calatrava Volcanic Field, central Spain). *Geochim. Cosmochim. Acta* 185, 477–497.

Lustrino, M., and Wilson, M. (2007). The circum-Mediterranean anorogenic Cenozoic igneous province. *Earth Sci. Rev.* 81, 1–65.

Marsh, B. D. (1996). Solidification fronts and magmatic evolution. *Mineral. Mag.* 60, 5–40.

Mattsson, H. B., Nandedkar, R. H., and Ulmer, P. (2013). Petrogenesis of the melilitic and nephelinitic rock suites in the lake Natron-Engaruka monogenetic volcanic field, northern Tanzania. *Lithos* 179, 175–192.

Matusiak-Malek, M., Ntaflos, T., Puziewicz, J., Woodland, A., Uenver-Thiele, L., and Lipa, D. (2018). From mantle to crust: variable origin of clinopyroxene from eastern limb of Central European Volcanic Province. *Geophys. Res. Abstracts* 20, EGU2018–EGU17407.

Mayer, B., Jung, S., Romer, R. L., Pfänder, J. A., Llügel, A., Pack, A., et al. (2014). Amphibole inalkaline basalts from intraplate settings: implications for the petrogenesis of alkaline lavas from the metasomatised lithospheric mantle. *Contrib. Mineral. Petrol.* 167:989.

Orejana, D., Villaseca, C., and Paterson, B. A. (2006). Geochemistry of pyroxenitic and hornblenditic xenoliths in alkaline lamprophyres from the Spanish Central System. *Lithos* 86, 167–196.

Peterson, T. D., and LeCheminant, A. N. (1993). Glimmerite xenoliths in early proterozoic ultrapotassic rocks from the Churchill province. *Canad. Mineral.* 31, 801–819.

Praegel, N. O. (1981). Origin of ultramafic inclusions and megacrysts in a monchiquite dyke at Streap, Inverness-shire, Scotland. *Lithos* 14, 305–322.

Raffone, N., Chazot, G., Pin, C., Vannucci, R., and Zanetti, A. (2009). Metasomatism in the lithospheric mantle beneath Middle Atlas (Morocco) and the origin of Fe- and Mg-rich wehrlites. *J. Petrol.* 50, 197–249.

Re, G., Palin, J. M., White, J. D. L., and Parolari, M. (2017). Unravelling the magmatic system beneath a monogenetic volcanic complex (Jagged Rocks Complex, Hopi Buttes, AZ, USA). *Contrib. Mineral. Petrol.* 172:94.

Reyes, J., Villaseca, C., Barbero, L., Quejido, A. J., and Santos Zalduegui, J. F. (1997). *Description of a Rb, Sr, Sm and Nd Separation Method for Silicate Rocks in Isotopic Studies*. Soria: I Congreso Ibérico de Geoquímica, 46–55.

Shaw, C. S. J., and Eyzaguirre, J. (2000). Origin of megacrysts in the mafic alkaline lavas of the West Eiffel volcanic field, Germany. *Lithos* 50, 75–95.

Sun, S. S., and McDonough, W. F. (1989). "Chemical and isotopic systematics of oceanic basalts: implications for mantle composition and processes", in Magmatism in ocean basins, eds A.D. Saunders, and M.J. Norry. *Geol. Soc. Spec. Publ.* 42, 313–345.

Ubide, T., Caulfield, J., Brandt, C., Bussweiler, Y., Mollo, S., Di Stefano, F., et al. (2019). Deep magma storage revealed by multi-method elemental mapping of clinopyroxene megacrysts at Stromboli volcano. *Front. Earth Sci.* 7:239.

Ubide, T., Galé, C., Larrea, P., Arranz, E., and Lago, M. (2014). Antecrysts and their effect on rock compositions: the Cretaceous lamprophyre suite in the Catalonian Coastal ranges (NE Spain). *Lithos* 20, 214–233.

Ulrych, J., Dostal, J., Adamovic, J., Jelínek, E., Spacek, P., Hegner, E., et al. (2011). Recurrent Cenozoic activity in the Bohemian Massif (Czech Republic). *Lithos* 123, 133–144.

Ulrych, J., Krmícek, L., Teschner, C., Skála, R., Adamovic, J., Durisová, J., et al. (2018). Chemistry and Sr-Nd isotope signature if aamphibole of the magnesio-hastingsite-pargasite-kaersutite series in Cenozoic volcanic rocks: insights into lithospheric mantle beneath the Bohemian Massif. *Lithos* 31, 308–321.

Vannucci, R., Piccardo, G. B., Rivalenti, G., Zanetti, A., Rampone, E., Ottolini, L., et al. (1995). Origin of LREE-depleted amphiboles in the subcontinental mantle. *Geochim. Cosmochim. Acta* 59, 1763–1771.

Villaseca, C., Ancochea, E., Orejana, D., and Jeffries, T. E. (2010). "Composition and evolution of the lithospheric mantle in central Spain: inferences from peridotite xenoliths from the Cenozoic Calatrava volcanic field", in Petrological evolution of the European Lithospheric Mantle, eds M. Coltorti, H., Downes, M., Grégoire, and S.Y. O'Reilly. *Geol. Soc. Spec. Publ. Lon.* 337, 125–151.

Villaseca, C., Dorado, O., and Orejana, D. (2019a). Mineral chemistry of megacryts and associated clinopyroxenite enclaves in the Calatrava Volcanic Field: crystallization processes in mantle magma chambers. *J. Iberian Geol.* 45, 401–426.

Villaseca, C., Belousova, E., Barfod, D., and González-Jiménez, J. M. (2019b). Dating metasomatic events in the lithospheric mantle beneath the Calatrava volcanic field (central Spain). *Lithosphere* 11, 192–208.

Wilkinson, J. F. G., and Stolz, A. J. (1997). Subcalcic clinopyroxenites and associated ultramafic xenoliths in alkali basalt near Glen Innes, northeastern New South Wales, Australia. *Contrib. Mineral. Petrol.* 127, 272–291.

Yu, X., Zeng, G., Chen, L. H., Hu, S. L., and Yu, Z. Q. (2019). Magma-magma interaction in the mantle recorded by megacrysts from cenozoic basalts in eastern China. *Int. Geol. Rev.* 61, 675–691.

Zindler, A., and Hart, S. R. (1986). Chemical geodynamics. *Annu. Rev. Earth Planet. Sci.* 14, 493–571.